Diptych varieties. I

Gavin Brown and Miles Reid *

Abstract

We present a new class of affine Gorenstein 6-folds obtained by smoothing the 1-dimensional singular locus of a reducible affine toric surface; their existence is established using explicit methods in toric geometry and serial use of Kustin–Miller Gorenstein unprojection. These varieties have applications as key varieties in constructing other varieties, including local models of Mori flips of Type A.

We introduce a large class of remarkable 6-folds called *diptych varieties*. Each is an affine 6-fold V_{ABLM} constructed starting from two toric 4-fold panels $V_{AB} \cup V_{LM}$ hinged along a reducible toric surface $T = V_{AB} \cap V_{LM}$ (compare the Wilton diptych [W]). The construction depends on discrete toric data called a *diptych of long rectangles*, that describe the monomial cone of the two toric panels V_{AB} and V_{LM}. It is equivariant under a big torus $\mathbb{T} = (\mathbb{G}_m)^4 = (\mathbb{C}^\times)^4$. Apart from easy initial cases, diptych varieties are indexed by 3 natural numbers d, e, k, or by a 2-step recurrent continued fraction $[d, e, d, \dots, (d \text{ or } e)]$ to k terms (Classification Theorem 3.3). Once this combinatorial data is set up, Main Theorem 1.1 guarantees the existence of the diptych variety. The worked example 1.2 illustrates almost all the main features of our construction. This paper is backed up by a website

`http://www-staff.lboro.ac.uk/~magdb/aflip.html`

that contains current drafts of Parts II–IV, together with computer algebra calculations, links to other papers and further auxiliary material.

Diptych varieties V_{ABLM} are designed for use as ambient spaces or *key varieties* in constructing other spaces, much as toric varieties. As discussed briefly in the final Section 6, our main motivation is their relation with the "continued division" algorithm [M], that Mori used to prove the existence of flips of Type A. Our work also overlaps with the more recent Gross–Hacking–Keel deformations of cycles of planes [GHK] in some cases where these lead to algebraic varieties.

Contents

*Partially funded by Korean Government WCU Grant R33-2008-000-10101-0

1 Introduction

This section gives rough statements of our main results and an outline plan of the paper. The extended example of 1.2 illustrates all the main ideas. We write $\mathbb{A}^n = \mathbb{C}^n$ for affine space, $\mathbb{G}_m = \mathbb{C}^\times$ for the multiplicative group and $\mathbb{T} = (\mathbb{C}^\times)^4$ for the 4-dimensional torus. Our main interest is in varieties over $\mathbb{C}$, although in the final analysis, our diptych varieties are defined as schemes over $\mathbb{Z}$.

1.1 Main results and overview of the paper

A *tent* is a reducible affine surface $T = S_0 \cup S_1 \cup S_2 \cup S_3$ as in Figure 1.1. Its four irreducible components are $S_0, S_2 \cong \mathbb{A}^2$ and S_1, S_3 cyclic quotient singularities of type $\frac{1}{r}(\alpha, 1)$ and $\frac{1}{s}(\beta, 1)$, where r, α are coprime natural numbers, and similarly for s, β. We glue the four toric surfaces transversally along their toric strata, giving T four 1-dimensional singular axes of transverse ordinary double points; the two axes on S_2 are the *top* axes of T, and the two on S_0 its *bottom* axes.

Section 2 recalls basic facts on toric geometry and studies certain deformations of tents. Our first result is Theorem 2.10: an extension $T \subset V_{AB}$ of a tent T to an affine toric 4-fold V_{AB} that smooths the top axes is determined by a matrix $\left(\begin{smallmatrix} r & a \\ b & s \end{smallmatrix}\right) \in \mathrm{SL}(2,\mathbb{Z})$ with $a, b \geq 0$ and $a \equiv \alpha \bmod r$, $b \equiv \beta \bmod s$. Corollary 2.8 gives an alternative statement in terms of *continued fraction expansions of* 0, obtained by concatenating with a 1 the expansions of *complementary* fractions $\frac{r}{\beta}$ and $\frac{r}{r-\alpha}$. This is routine material in toric geometry, but the

basic results and detailed notation for the monomial cone σ_{AB} introduced here are in use throughout the paper.

Section 3 treats our first substantial result, Classification Theorem 3.3, classifying diptychs of toric extensions $T \subset V_{AB}$ and $T \subset V_{LM}$ that smooth respectively the top and bottom axes of T. By Lemma 3.2, the numerical conditions on T for the second smoothing to exist is a second matrix $\left(\begin{smallmatrix} r & g \\ h & s \end{smallmatrix}\right) \in \mathrm{SL}(2,\mathbb{Z})$ with $ag \equiv 1 \bmod r$ and $bh \equiv 1 \bmod s$. Theorem 3.3 classifies all solutions to this problem: with simple initial exceptions, each corresponds to a 2-step recurrent continued fraction $[d, e, d, \ldots, (d \text{ or } e)]$. Theorem 3.3 is proved by a simple descent argument.

At this point we introduce a case division (we discuss the necessity for this briefly in Section 6). The *main case* is $d, e \geq 2$ and $de > 4$; we concentrate our efforts primarily on this case in the rest of the current paper. The other cases involve some new features, and their proofs require minor modifications; they are as follows:

- $de \leq 3$. This involves only a small number of quite small cases, and we deal with them in an appendix to [BR2].
- The cases $d = e = 2$ and $d = 1$, $e = 4$ are treated in [BR2]. There are two infinite series of varieties with a convincing standard quasihomogeneous structure.
- d or $e = 1$ and $de > 4$. This case requires a proof that is basically on the same scale as the main case; we relegate the details to [BR3] to avoid excessive repetition, bulky notation, and many case divisions.

Diptychs serve as the input to our Main Theorem, the existence of diptych varieties:

Theorem 1.1 *A diptych of 4-fold toric panels $T \subset V_{AB}$ and $T \subset V_{LM}$ that smooth respectively the top and bottom axes of T extends to a 6-fold V_{ABLM}:*

$$\begin{array}{ccc} T & \subset & V_{AB} \\ \bigcap & & \bigcap \\ V_{LM} & \subset & V_{ABLM} \end{array} \tag{1.1}$$

The diptych variety *V_{ABLM} is an affine variety with an action of the torus $\mathbb{T} = (\mathbb{G}_m)^4$. It has a regular sequence A, B, L, M consisting of eigenfunctions of the $\mathbb{T}$-action such that V_{AB} and V_{LM} are the sections given by $L = M = 0$ and $A = B = 0$, with T their intersection $A = B = L = M = 0$.*

It follows that V_{ABLM} is a Gorenstein affine 6-fold and is a flat 4-parameter deformation of the tent T. The $\mathbb{T}$-action restricts to the big torus of both 4-fold panels V_{AB} and V_{LM}; the original tent T is a union of toric strata in each, with the $\mathbb{T}$-action inducing the natural $(\mathbb{G}_m)^2$ action on each of its four toric components.

Section 4 lays the groundwork for the proof in Section 5. The main idea is to exploit the relation between the monomial lattices and the monomial cones of the two different toric

varieties V_{AB} and V_{LM} to deduce important consequences for monomials in the coordinate ring of the diptych variety V_{ABLM}. Our proof of Main Theorem 1.1 in Section 5 makes essential use of convexity properties of these monomials (illustrated in the Pretty Polytope of Figure 4.1) and congruence properties (the Padded Cell of Figure 4.3).

Section 5 proves Theorem 1.1 in the main case by *serial unprojection*. We start from two equations defining a codimension 2 complete intersection $V_0 \subset \mathbb{A}^8_{\langle x_0,x_1,y_0,y_1,A,B,L,M\rangle}$, and adjoin the remaining variables one at a time by unprojection $V_{\nu+1} \to V_\nu$. Section 5.2 determines the *unprojection order* in which we must adjoin the variables $x_2, \dots, y_l$. It is inverse to the order of elimination (or projection) of variables from the toric panel V_{AB}, corresponding to the concatenated continued fraction $[a_2, \dots, a_k, b_l, \dots, b_1] = 0$. Serial use of the Kustin–Miller unprojection theorem of [PR] provides most of what we need.

Extended Example 1.2 is the case corresponding to the recurrent continued fraction $[2, 4, 2]$ or the expansion of zero $[4, 2, 1, 3, 2, 2] = 0$. We use a beautiful trick with Pfaffians to compute the sequence of unprojection variables $[x_2, y_2, y_3, x_3, y_4]$ as rational functions with specified poles, the geometric interpretation of Kustin–Miller unprojection. This example illustrates all but one of the main points, and exemplifies our strategy of handling a diptych variety V_{ABLM} as an explicit object, but without necessarily writing down all the relations for its coordinate ring, much as for a toric variety.

The extended example glosses over one logical point that is the key issue for most of Sections 4–5. Each step $V_{\nu+1} \to V_\nu$ of the induction must set up a new unprojection divisor $D_\nu \subset V_\nu$. The divisor D_ν itself is the product of a monomial curve $A^\alpha B^\beta = 0$ with an affine space $\mathbb{A}^4_{\langle x_i,y_j,L,M\rangle}$, but we still have to prove it is a subscheme of V_ν.

1.2 Extended example

1.2.1 Background and notation

For $r > 0$ and a coprime to r, we write $\frac{1}{r}(1, a)$ for the action of $\mathbb{Z}/r$ on $\mathbb{A}^2$ given by $(u, v) \mapsto (\varepsilon u, \varepsilon^a v)$ where $\varepsilon = \exp \frac{2\pi i}{r} \in \mathbb{C}$ is a chosen primitive rth root of 1. We use the same notation for the cyclic quotient singularity $\mathbb{A}^2/(\mathbb{Z}/r) = \operatorname{Spec} \mathbb{C}[u, v]^{\mathbb{Z}/r}$. We focus here on concrete cases, starting with $\frac{1}{7}(1, 2)$; the ring of invariants $\mathbb{C}[u, v]^{\mathbb{Z}/7}$ is generated by the monomials

$$y_0 = u^7, \quad y_1 = u^5 v, \quad y_2 = u^3 v^2, \quad y_3 = uv^3, \quad y_4 = v^7, \tag{1.2}$$

with relations between them determined by the *tag equations*

$$y_0 y_2 = y_1^2, \quad y_1 y_3 = y_2^2, \quad y_2 y_4 = y_3^3. \tag{1.3}$$

These are of the general form $v_{i-1} v_{i+1} = v_i^{a_i}$ for any 3 consecutive monomials v_{i-1}, v_i, v_{i+1} on the Newton boundary. The exponents or *tags* a_i are the entries in the Jung–Hirzebruch continued fraction expansion of $\frac{r}{r-a}$; here $\frac{7}{7-2} = 2 - \frac{1}{2-\frac{1}{3}} = [2, 2, 3]$. The quotient $\mathbb{A}^2 \to S \subset \mathbb{A}^5_{\langle y_{0\dots4}\rangle}$ is thus the morphism $(u, v) \mapsto (y_{0\dots4})$, and the image S is uniquely determined by (1.3): the complete intersection (1.3) consists of S plus the (y_0, y_4)-plane with a "fat"

nonreduced structure. To see actual generators of the ideal I_S we also need the "long equations" $y_0y_3 = y_1y_2$, $y_1y_4 = y_2y_3^2$ and $y_0y_4 = y_1y_3^2$, that derive from (1.3) using easy syzygy manipulations. In what follows, we write $S = S_3$ for the quotient $\frac{1}{7}(1,2)$.

In the same way, the quotient singularity $\frac{1}{7}(1,3)$ is

$$S_1 \subset \mathbb{A}^4_{\langle x_0,x_1,x_2,x_3\rangle} \quad \text{given by} \quad x_0x_2 = x_1^2, \quad x_1x_3 = x_2^4 \tag{1.4}$$

with $[2,4] = 2 - \frac{1}{4} = \frac{7}{4}$.

1.2.2 The tent T

The starting point for our example is the reducible affine surface or *tent* of Figure 1.1 (with $k = 3$, $l = 4$ and $k + l + 2 = 9$ in our case). It consists of a cycle of 4 components,

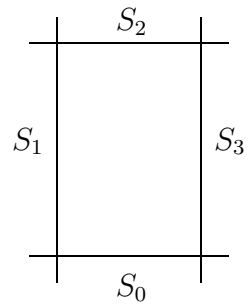

Figure 1.1: The tent $T = S_0 \cup S_1 \cup S_2 \cup S_3 \subset \mathbb{A}^{k+l+2}_{\langle x_{0\dots k}, y_{0\dots l}\rangle}$ is obtained by glueing $S_0 \cup S_1$ transversally along the x_0-axis, $S_1 \cup S_2$ along the x_k-axis, $S_2 \cup S_3$ along the y_l-axis, and $S_3 \cup S_0$ along the y_0-axis

with vertical sides the surface quotient singularities $S_1 \subset \mathbb{A}^4_{\langle x_{0\dots k}\rangle}$ and $S_3 \subset \mathbb{A}^5_{\langle y_{0\dots l}\rangle}$ of types $\frac{1}{7}(1,3)$ and $\frac{1}{7}(1,2)$ as just described, and top and bottom the coordinate planes $S_2 = \mathbb{A}^2_{\langle x_k,y_l\rangle}$ and $S_0 = \mathbb{A}^2_{\langle x_0,y_0\rangle}$. In equations, $T \subset \mathbb{A}^9$ is the reducible variety defined by

$$I_{S_1}, I_{S_3} \quad \text{and} \quad x_iy_j = 0 \quad \text{for all } i,j \text{ with } (i,j) \neq (0,0),(k,l). \tag{1.5}$$

1.2.3 First toric extension $T \subset V_{AB}$

We now seek to embed T into a toric variety V (irreducible and normal) so that T is both a regular section of V and a union of toric strata.

One solution is the affine toric 4-fold V_{AB} with monomial cone schematically represented in Figure 1.2, our first *long rectangle*. It is a schematic representation of a cone $\sigma(V_{AB})$, the Newton polygon of V_{AB} in the monomial lattice $\mathbb{M} = \mathbb{Z}^4$. We read $\sigma(V_{AB})$ and the toric variety V_{AB} automatically from the figure as follows: the dots around the boundary (clockwise from bottom left) are the generators $x_{0\dots k}$, $y_{l\dots 0}$; the two remaining generators A, B are shown as *annotations* at the top corners. We also draw them in their correct geometric position in the 4-dimensional lattice $\mathbb{M}$ in Figure 2.3, but this long rectangle shorthand is usually more convenient. The relations (1.3) and (1.4) continue to

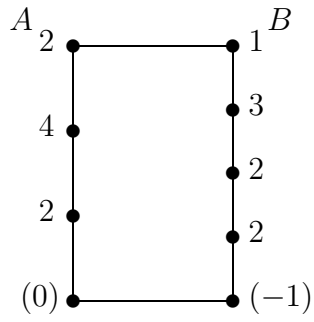

Figure 1.2: The long rectangle for V_{AB}

hold, as represented by the tags down the long sides. These constrain $x_{0\ldots k}$ to a plane face of $\sigma(V_{AB})$, and in that plane they generate the Newton boundary of $\frac{1}{7}(1,4)$; ditto $y_{0\ldots l}$. The new ingredients are the tags and annotations ${}^A2, 1^B$ at the top corners, that say how we intend to deform the reducible equations $x_2y_4 = 0$ and $x_3y_3 = 0$ for T appearing in (1.5) to usual binomial equations of toric geometry:

$$x_2y_4 = x_3^2A, \quad x_3y_3 = y_4B. \tag{1.6}$$

We view A and B as deformation parameters, and interpret (1.6) as smoothing the reducible double locus along the x_3- and y_4-axes, the top corners $S_1 \cap S_2$ and $S_2 \cap S_3$ of Figure 1.1.

On the other hand, equations (1.6) and the original tag equations (1.3–1.4) now completely determine the cone $\sigma(V_{AB})$ in a monomial lattice $\mathbb{M} = \mathbb{Z}^4$. Indeed, x_3, y_4, A, B is a $\mathbb{Z}$-basis of $\mathbb{M}$, and the remaining generators $x_2, \ldots, x_0$, $y_3, \ldots, y_0$ are Laurent monomials in this basis, obtained by *continued division* from (1.6) together with (1.3–1.4):

$$\begin{aligned} x_2 &= x_3^2(Ay_4^{-1}), & y_3 &= y_4(Bx_3^{-1}), \\ x_1 &= x_3^7(Ay_4^{-1})^4, & y_2 &= y_4^2(Bx_3^{-1})^3, \\ x_0 &= x_3^{12}(Ay_4^{-1})^7, & y_1 &= y_4^3(Bx_3^{-1})^5, \\ & & y_0 &= y_4^4(Bx_3^{-1})^7. \end{aligned} \tag{1.7}$$

A rational polyhedral cone σ in the monomial lattice $\mathbb{M}$ defines a irreducible, normal toric variety $V_{\mathbb{M},\sigma} = \operatorname{Spec}\mathbb{C}[\mathbb{M} \cap \sigma]$. We claim more: our monomials $x_{0\ldots3}, y_{0\ldots4}, A, B$ in $\mathbb{M}$ generate $\mathbb{M} \cap \sigma_{AB}$, and the resulting toric variety $V_{AB} = \operatorname{Spec}\mathbb{C}[\mathbb{M} \cap \sigma_{AB}]$ is a flat deformation of T. When we say deformation, we mean the total space of the deformation; in fact A, B define a flat morphism $V_{AB} \to \mathbb{A}^2_{\langle A,B\rangle}$ with fibre $T : (A = B = 0)$ over 0, although this morphism does not figure prominently in our considerations.

The relations satisfied by our monomials come implicitly from their inclusion in $\mathbb{M}$. We are usually not interested in writing them all out, but we want to find enough equations to justify our claim. By substituting from (1.7), we find the relation

$$x_1y_0 = A^4B^7 \tag{1.8}$$

that deforms the original equation $x_1y_0 = 0$ in T; this is the *corner tag* (0) of Figure 1.2, indicating a tag equation at x_0, with tag 0 derived from the other tags (the annotation

A^4B^7 is left implicit). We view it as a partial smoothing of the reducible double locus of T along the x_0-axis – (1.8) of course defines a normal hypersurface in $\mathbb{A}^4_{\langle x_1,y_0,A,B\rangle}$

Now, how does the relation $x_0y_1 = 0$ deform? From (1.7) we write out $x_0y_1 = x_3^7y_4^{-4}A^7B^5$, hence

$$x_0y_1 = y_0^{-1}A^7B^{12} \quad \text{or} \quad x_0y_1 = x_1A^3B^5. \tag{1.9}$$

The first equality is a tag equation for y_0, with negative tag -1; this is the (-1) at the bottom right of Figure 1.2. Along the y_0-axis of T, where $y_0 \neq 0$, (1.9) ensures that the A, B deformation is also a partial smoothing of the singularity, making it irreducible and normal. However, (1.9) with its negative tag is anomalous in that it is not a polynomial equation, so we are not really allowed to use it as a generator of the ideal of the affine variety V_{AB}. We thus replace it by the second expression, which in view of (1.8) is equivalent to it where $y_0 \neq 0$. The relation $x_0y_1 = x_1A^3B^5$ is also anomalous as a tag equation for y_0, since it involves the "opposite" generator x_1 in place of y_0. Now the equations of V_{AB} include (1.8–1.9); these define an irreducible normal complete intersection in $\mathbb{A}^6_{\langle x_0,x_1,y_0,y_1,A,B\rangle}$.

Since V_{AB} is a toric 4-fold, it is Cohen–Macaulay; we see in Lemma 2.3 that it is also Gorenstein. (Or one checks directly from the description above that the semigroup ideal of interior monomials of $\sigma(V_{AB})$ is generated by AB; compare 2.3 and Figure 2.3.) One checks that the locus $(A = B = 0)$ inside V_{AB} equals T at the general point of each component, and in particular each component is 2-dimensional. Therefore A, B is a regular sequence and $T \subset V_{AB}$ is a flat deformation.

1.2.4 Conclusion

In this example we found the A, B deformation $T \subset V_{AB}$ in a more-or-less inevitable way starting from the new tag equations $x_2y_4 = x_3^2A$ and $x_3y_3 = y_4B$, that naturally smooth the double locus of T along the x_3- and y_4-axes. After a monomial calculation that is birationally forced, our rectangle closed up neatly to give the tag equations (1.8–1.9), so that this deformation also leads to partial smoothings of the x_0 and y_0-axes, giving an irreducible and normal variety V_{AB} such that $A = B = 0$ contains S_0 as a reduced component. Corollary 2.8 explains that this miracle works precisely because the concatenation $[4, 2, 1, 3, 2, 2]$ is a *continued fraction expansion of* 0. These numbers are the tags at $x_2, x_3, y_4, \dots, y_1$; the asymmetry ($x_1$ omitted but y_1 included) is significant, and relates to the anomalous tag equations (1.9).

1.2.5 Second toric extension $T \subset V_{LM}$

As hinted above, T has more than one deformation to a toric 4-fold. We now write down the second long rectangle Figure 1.3 and the resulting deformation $T \subset V_{LM}$. The calculations are just as for V_{AB}, except that we start from the bottom and work up. Hindsight based on Corollary 2.8 and $[3, 2, 2, 1, 4, 2] = 0$ tells us that this will work. The new tag equations that smooth out the x_0- and y_0-axes of T are represented by the ${}_L4, 1_M$

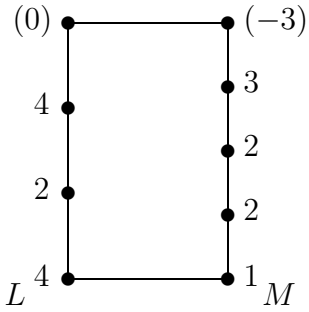

Figure 1.3: The long rectangle for V_{LM}

at the bottom:

$$x_1 y_0 = x_0^4 L, \quad x_0 y_1 = y_0 M. \tag{1.10}$$

This time x_0, y_0, L, M base the monomial lattice and (1.10) together with (1.3–1.4) give the remaining variables as Laurent monomials:

$$\begin{aligned} x_1 &= x_0^4 (L y_0^{-1}), & y_1 &= y_0 (M x_0^{-1}), \\ x_2 &= x_0^7 (L y_0^{-1})^2, & y_2 &= y_0 (M x_0^{-1})^2, \\ x_3 &= x_0^{24} (L y_0^{-1})^7, & y_3 &= y_0 (M x_0^{-1})^3, \\ & & y_4 &= y_0^2 (M x_0^{-1})^7. \end{aligned} \tag{1.11}$$

As before, we deduce the tag equations for x_3 and y_4:

$$x_2 y_4 = L^2 M^7, \quad x_3 y_3 = y_4^{-3} L^7 M^{27} = x_2^3 L M^3. \tag{1.12}$$

The latter is anomalous as before: the partial smoothing along the y_4-axis is specified either by the Laurent monomial y_4^{-3} or by a polynomial equation x_2^3 in the "opposite" variable x_2.

1.2.6 The 6-fold V_{ABLM}

We now have two deformations $T \subset V_{AB}$ and $T \subset V_{LM}$ of our tent T to toric 4-folds; we call this a *diptych of toric deformations*. The two panels are quite different: V_{AB} is smooth along the x_3- and y_4-axes by (1.6), but has hypersurface singularities along the x_0- and y_0-axes of transverse type $x_1 y_0 = A^4 B^7$ and $x_0 y_1 = y_0^{-1} A^7 B^{12}$ by (1.8) and (1.9). In contrast, V_{LM} smooths the x_0- and y_0-axes by (1.10), but leaves the x_3- and y_4-axes with the transverse hypersurface singularities $x_2 y_4 = L^2 M^7$ and $x_3 y_3 = y_4^{-3} L^7 M^{27}$ of (1.12).

Theorem 1.1 now asserts that these two toric panels fit together in a 4-parameter deformation $T \subset V_{ABLM}$:

$$\begin{array}{ccc} T & \subset & V_{AB} \\ \bigcap & & \bigcap \\ V_{LM} & \subset & V_{ABLM} \end{array} \tag{1.13}$$

More precisely, we build an affine 6-fold V_{ABLM} with a regular sequence A, B, L, M such that the section $L = M = 0$ is V_{AB} and $A = B = 0$ is V_{LM}. The idea is amazingly naive: starting at the top, we simply merge the tag equations (1.6) and (1.12) for x_3 and y_4 from V_{AB} and V_{LM}, obtaining $W \subset \mathbb{A}^8_{\langle x_2,x_3,y_4,y_3,A,B,L,M\rangle}$ defined by

$$x_2y_4 = x_3^2A + L^2M^7, \quad x_3y_3 = y_4B + x_2^3LM^3. \tag{1.14}$$

It is a codimension 2 complete intersection, A, B, L, M is a regular sequence for W, and the section $L = M = 0$ is birational to V_{AB} by the Laurent monomial argument of (1.7).

The plan is now to adjoin x_1, x_0, y_2, y_1, y_0 as rational functions on W, so V_{ABLM} will be birational to W. In commutative algebra terms, the coordinate ring of V_{ABLM} is constructed from the complete intersection (1.14) by *serial unprojection*. We run through the construction as a pleasant narrative; the reasons it all works include some detailed tricks that we explain later when we treat the material more formally. Suffice it to say that we add the new variables x_1, x_0, y_2, y_1, y_0 one at a time, *and in that order*. Adding them in a different order does not work.

1.2.7 First pentagram

We construct x_1 as a rational function on W (1.14) with divisor of poles the codimension 3 complete intersection

$$D : (x_3 = y_4 = LM^3 = 0) \subset W, \tag{1.15}$$

where LM^3 is the hcf of the two terms L^2M^7 and $x_2^3LM^3$ in (1.14). The new variable x_1 appears in three equations

$$x_1x_3 = \cdots, \quad x_1y_4 = \cdots, \quad x_1LM^3 = \cdots, \tag{1.16}$$

that express the rational function x_1 as a homomorphism $\mathcal{I}_D \to \mathcal{O}_W$. More intrinsically, x_1 is an *unprojection variable* $x_1 \in \mathcal{H}om(\mathcal{I}_D, \omega_W)$ with Poincaré residue a basis of $\omega_D \cong \mathcal{O}_D$; see [PR] and [Ki] for the theory and practice of unprojection. In our calculation we take as input the equations (1.14) and (1.15) of W and D, and use them to fix up a 5×5 skew matrix $A = \{a_{ij}\}$ whose five 4×4 Pfaffians are the two input equations (1.14) and the three new unprojection equations (1.16) for x_1. This calculation is repeated serially in what follows, and we make it systematic with *magic pentagrams*:

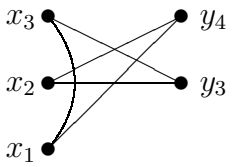

$$\begin{pmatrix} y_3 & x_2^3 & -B & -x_1 \\ & y_4 & LM^3 & -x_3A \\ & & x_3 & LM^4 \\ & & & x_2 \end{pmatrix} \tag{1.17}$$

$$\begin{aligned} 23.45 \quad & x_2y_4 = x_3^2A + L^2M^7, \\ 12.34 \quad & x_3y_3 = y_4B + x_2^3LM^3, \end{aligned}$$

$$\begin{aligned} 12.35 \quad & x_1y_4 = x_2^3x_3A + y_3LM^4, \\ 13.45 \quad & x_1x_3 = x_2^4 + BLM^4, \\ 12.45 \quad & x_2y_3 = x_3AB + x_1LM^3. \end{aligned}$$

The array is a skew 5×5 matrix $A = \{a_{ij}\}$; we only write the 10 upper-triangular entries $a_{12} = y_3, \dots, a_{15} = -x_1$, etc. Its 4×4 Pfaffians are

$$\mathrm{Pf}_{ij.kl} = a_{ij}a_{kl} - a_{ik}a_{jl} + a_{il}a_{jk} \quad \text{for any distinct } i, j, k, l \tag{1.18}$$

(as with minors and cofactors, with an overall choice of ± 1; in long calculations we abbreviate $\mathrm{Pf}_{ij.kl}$ to $ij.kl$). In (1.17), viewing y_3, y_4, x_3, x_2 and the two equations $x_2y_4 = \cdots$, $x_3y_3 = \cdots$ as given, we seek to add x_1 and three new equations $x_1x_3 = \cdots$, $x_1y_4 = \cdots$ and $x_2y_3 = \cdots + x_1LM^3$. These trinomial equations play a role for V_{ABLM} similar to the binomial tag equations $v_{i-1}v_{i+1} = v_i^{a_i}$ for the cyclic quotient singularities S_i and the tent T. The array is written out automatically from the pentagram and the given equations (1.14): we write the given variables y_3, y_4, x_3, x_2 down the superdiagonal, the new unprojection variable x_1 in the top right, and the given $LM^3 = \mathrm{hcf}(L^2M^7, x_2^3LM^3)$ as the entry a_{24}. Requiring $\mathrm{Pf}_{12.34}$ and $\mathrm{Pf}_{23.45}$ to give (1.14) determines the remaining entries. The output is the three equations involving x_1 as the three remaining Pfaffians in (1.17).

1.2.8 Serial pentagrams

The remaining variables x_0, y_2, y_1, y_0 are adjoined likewise to give the codimension 7 variety V_{ABLM} (see Section 5 for a formal treatment). We write out the calculations without further comment for your delight.

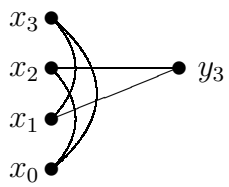

$$\begin{pmatrix} y_3 & x_1 & -AB & -x_0 \\ & x_3 & LM^3 & -x_2^3 \\ & & x_2 & BM \\ & & & x_1 \end{pmatrix}$$

23.45 $\quad x_1x_3 = x_2^4 + BLM^4,$
12.34 $\quad x_2y_3 = ABx_3 + LM^3x_1,$

12.35 $\quad x_0x_3 = x_1x_2^3 + BMy_3,$
13.45 $\quad x_0x_2 = x_1^2 + AB^2M,$
12.45 $\quad x_1y_3 = ABx_2^3 + LM^3x_0.$

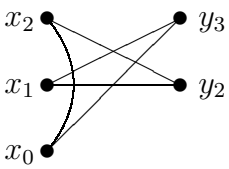

$$\begin{pmatrix} y_3 & LM^2x_0 & -ABx_2^2 & -y_2 \\ & x_2 & M & -x_1 \\ & & x_1 & AB^2 \\ & & & x_0 \end{pmatrix}$$

23.45 $\quad x_0x_2 = x_1^2 + AB^2M,$
12.34 $\quad x_1y_3 = ABx_2^3 + LM^3x_0,$

12.35 $\quad x_2y_2 = AB^2y_3 + LM^2x_0x_1,$
13.45 $\quad x_1y_2 = A^2B^3x_2^2 + LM^2x_0^2,$
12.45 $\quad x_0y_3 = ABx_1x_2^2 + My_2.$

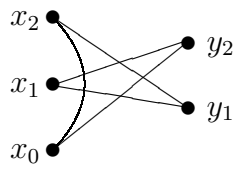

$$\begin{pmatrix} y_2 & LMx_0^2 & -A^2B^3x_2 & -y_1 \\ & x_2 & M & -x_1 \\ & & x_1 & AB^2 \\ & & & x_0 \end{pmatrix}$$

$$\begin{aligned} 23.45 \quad & x_0x_2 = x_1^2 + AB^2M, \\ 12.34 \quad & x_1y_2 = A^2B^3x_2^2 + LM^2x_0^2, \end{aligned}$$

$$\begin{aligned} 12.35 \quad & x_2y_1 = AB^2y_2 + LMx_0^2x_1, \\ 13.45 \quad & x_1y_1 = A^3B^5x_2 + LMx_0^3, \\ 12.45 \quad & x_0y_2 = A^2B^3x_1x_2 + My_1. \end{aligned}$$

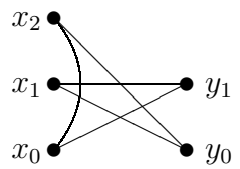

$$\begin{pmatrix} y_1 & Lx_0^3 & -A^3B^5 & -y_0 \\ & x_2 & M & -x_1 \\ & & x_1 & AB^2 \\ & & & x_0 \end{pmatrix}$$

$$\begin{aligned} 23.45 \quad & x_0x_2 = x_1^2 + AB^2M, \\ 12.34 \quad & x_1y_1 = A^3B^5x_2 + LMx_0^3, \end{aligned}$$

$$\begin{aligned} 12.35 \quad & x_2y_0 = AB^2y_1 + Lx_0^3x_1, \\ 13.45 \quad & x_1y_0 = A^4B^7 + Lx_0^4, \\ 12.45 \quad & x_0y_1 = A^3B^5x_1 + My_0. \end{aligned}$$

The final two equations $x_1y_0 = \cdots$ and $x_0y_1 = \cdots$ merge the tag equations (1.8–1.9) and (1.10) for x_0 and y_0 at the bottom of the two long rectangles in exactly the same way as (1.14) merged the tag equations at the top. In other words, the whole calculation could have been done starting with these two equations and working up – if you liked the puzzle, you will enjoy turning it upside down and doing it all over again.

2 Toric partial smoothings of tents

This chapter centres around the combinatorics of continued fractions. After recalling standard facts, we define a tent T, and, under appropriate assumptions, construct a toric extension $T \subset V_{AB}$ that smooths its top two axes. The toric variety $T \subset V_{AB}$ can be treated in terms of a matrix $\left(\begin{smallmatrix} r & a \\ b & s \end{smallmatrix}\right) \in \mathrm{SL}(2, \mathbb{Z})$, or equivalently, in terms of a certain continued fraction expansion of 0. We use the latter treatment in 5.2 to understand V_{AB} by a sequence of Gorenstein projections.

2.1 Jung–Hirzebruch continued fractions

A *continued fraction expansion* is a formal expression

$$\begin{aligned} [c_1, \ldots, c_n] &= c_1 - 1/(c_2 - 1/(c_3 - \cdots - 1/c_n) \cdots) \\ &= c_1 - \frac{1}{c_2 - \frac{1}{\cdots - \frac{1}{c_n}}} = c_1 - \frac{1}{[c_2, \ldots, c_n]} \end{aligned} \tag{2.1}$$

The entries c_i are called *tags*. If $c_1, \ldots, c_n$ are integers, the righthand side is a rational number, provided that the expression makes sense, that is, division by zero does not occur. (The notation is explained in Riemenschneider [R] §3, pp. 220–3.)

The next proposition discusses four aspects of continued fractions. We spell out this material, because we use it often and with large multiplicity in what follows: we invert continued fractions and pass to complementary fractions, we "top and tail" them by cutting off a tag at one end and adding one at the other, say:

$$[a_0, \ldots, a_{k-1}] \mapsto [a_k, a_{k-1}, \ldots, a_1], \quad \text{etc.}, \tag{2.2}$$

and we concatenate the resulting fractions.

Proposition 2.1 **(a) Factoring a matrix:** *The formal identity*

$$\begin{pmatrix} 0 & 1 \\ -1 & c_1 \end{pmatrix} \begin{pmatrix} 0 & 1 \\ -1 & c_2 \end{pmatrix} \cdots \begin{pmatrix} 0 & 1 \\ -1 & c_n \end{pmatrix} = \begin{pmatrix} -q' & q \\ -p' & p \end{pmatrix}. \tag{2.3}$$

holds in indeterminates or variables $c_1, \ldots, c_n$, where p, q, p', q' are polynomials, the numerators and denominators of $p/q = [c_1, \ldots, c_n]$ and $p'/q' = [c_1, \ldots, c_{n-1}]$. (No cancellation occurs in the fraction p/q, whatever the nature or values of the quantities c_i, because p and q satisfy an hcf *identity $\alpha p + \beta q = 1$.) The fraction p'/q' is the* first convergent *of p/q.*

(b) Blowdown: $[c_1, \ldots, c_{n-1}, 1] = [c_1, \ldots, c_{n-1} - 1]$ *and*

$$[c_1, \ldots, c_{i-1}, 1, c_{i+1}, \ldots, c_n] = [c_1, \ldots, c_{i-1} - 1, c_{i+1} - 1, \ldots, c_n]. \tag{2.4}$$

This is just the identity $\left(\begin{smallmatrix} 0 & 1 \\ -1 & a \end{smallmatrix}\right)\left(\begin{smallmatrix} 0 & 1 \\ -1 & 1 \end{smallmatrix}\right)\left(\begin{smallmatrix} 0 & 1 \\ -1 & b \end{smallmatrix}\right) = \left(\begin{smallmatrix} 0 & 1 \\ -1 & a-1 \end{smallmatrix}\right)\left(\begin{smallmatrix} 0 & 1 \\ -1 & b-1 \end{smallmatrix}\right)$.

Two notions of "inverse" of a continued fraction play a role in our theory:

(c) Reciprocal: $[c_1, \ldots, c_n] = p/q$ *and its* reciprocal *continued fraction*

$$[c_n, \ldots, c_1] = p/q^* \tag{2.5}$$

share the same numerator p, and their denominators are inverse modulo p. More precisely, there is a formal identity

$$qq^* = N(c_2, \ldots, c_{n-1}) \cdot p + 1, \tag{2.6}$$

where $N(c_2, \ldots, c_{n-1})$ is the numerator of $[c_2, \ldots, c_{n-1}]$. In particular, if $c_i \in \mathbb{Z}$ and the expressions are meaningful then $[c_n, \ldots, c_1] = p/q^*$, where $qq^* \equiv 1 \bmod p$. See (2.11) *for what this means in our context.*

(d) Complement: *Let $p/q = [c_1, \ldots, c_n]$ with $c_i \in \mathbb{Z}$ and $c_i \geq 2$. Then the* complementary *continued fraction is $[b_1, \ldots, b_m] = p/(p-q)$, and satisfies*

$$[c_n, \ldots, c_1, 1, b_1, \ldots, b_m] = 0. \tag{2.7}$$

Moreover, serial blowdown reduces the expansion to $[1, 1] = [0] = 0$; in particular, $\sum(c_i - 1) = \sum(b_j - 1)$, and one of $b_1, c_1 \leq 2$. For example,

$$[4, \underline{2, 1, 3}, 2, 2] = [\underline{4, 1, 2}, 2, 2] = [\underline{3, 1, 2}, 2] = [\underline{2, 1, 2}] = [1, 1] = 0. \tag{2.8}$$

Remark 2.2 Traditionally, one uses Jung–Hirzebruch continued fractions to write a fraction $\frac{r}{a}$ with $r > a \geq 1$ and a, r coprime integers as

$$\frac{r}{a} = [b_1, \dots, b_{n-1}] = b_1 - \frac{1}{b_2 - \cdots}.$$

Then b_1 is the round-up $b_1 = \lceil \frac{r}{a} \rceil$, and is ≥ 2, because $\frac{r}{a} > 1$, and for the same reason all subsequent $b_i \geq 2$ (to the end of the algorithm). Here we do something slightly bigger, with $a \geq 1$, but $r \in \mathbb{Z}$ any integer coprime to a: for example, $\frac{-24}{7} = -3 - \frac{3}{7} = [-3, 3, 2, 2]$. This means that $b_1 = \lceil \frac{r}{a} \rceil \in \mathbb{Z}$; however, from the second step onwards and to the end of the algorithm, $1/(b_1 - \frac{r}{a}) > 1$ is a conventional fraction, so that $b_i \geq 2$ for each i with $2 \leq i \leq n-1$.

In traditional use, (2.3) identifies 3 types of data: a rational fraction $p/q > 1$, a continued fraction $[c_1, \dots, c_n]$ with all $c_i \geq 2$, and a matrix $\left(\begin{smallmatrix} -q' & q \\ -p' & p \end{smallmatrix}\right) \in \mathrm{SL}(2, \mathbb{Z})$ with $p > q > 0$. However, we relax these restrictions, considering things like $[5, 1, 3] = 5 - \frac{3}{2} = \frac{7}{2} = [4, 2]$ (a blowdown) or $[2, 0, 2] = 4$, with

$$\begin{pmatrix} 0 & 1 \\ -1 & 2 \end{pmatrix} \begin{pmatrix} 0 & 1 \\ -1 & 0 \end{pmatrix} \begin{pmatrix} 0 & 1 \\ -1 & 2 \end{pmatrix} = \begin{pmatrix} 0 & 1 \\ -1 & 2 \end{pmatrix} \begin{pmatrix} -1 & 2 \\ 0 & -1 \end{pmatrix} = \begin{pmatrix} 0 & -1 \\ 1 & -4 \end{pmatrix}. \tag{2.9}$$

The matrix product (2.3) is meaningful even when (2.1) involves division by zero. More generally, the sequence of integer tags $[c_1, \dots, c_n]$ contains more information than the matrix (2.3), which contains more information than the fraction $\frac{p}{q}$: while $\left(\begin{smallmatrix} -q' & q \\ -p' & p \end{smallmatrix}\right) \in \mathrm{SL}(2, \mathbb{Z})$, the fraction $\frac{p}{q}$ (when defined) is its image in the quotient group $\mathrm{PSL}(2, \mathbb{Z})$, whereas the expression $[c_1, \dots, c_n]$ is a lift to the "universal cover" of $\mathrm{SL}(2, \mathbb{Z})$ inside the universal cover of $\mathrm{SL}(2, \mathbb{R})$, keeping track of winding number. For example, $[0, 0, 0, 0]$ is the composite of 4 rotations by $\pi/2$, or $\left(\begin{smallmatrix} 0 & 1 \\ -1 & 0 \end{smallmatrix}\right)^4 = \mathrm{id}$. Running around one of our long rectangles below always gives winding number 1.

Notation for the quotient $\frac{1}{r}(\alpha, 1)$ As in Example 1.2, for $r \geq 1$ and $0 < \alpha \leq r$ coprime to r we write $\frac{1}{r}(\alpha, 1)$ for the $\mathbb{Z}/r$ action on $\mathbb{A}^2_{\langle u,v \rangle}$ given by $(u, v) \mapsto (\varepsilon^\alpha u, \varepsilon v)$, and for the quotient $S = \mathbb{A}^2/\frac{1}{r}(\alpha, 1)$ by this action. We allow $\mathbb{A}^2$ as the case $r = 1$, without worrying unduly about the value of α (of course, $\alpha = 0$); it corresponds to the identity matrix or the empty continued fraction $[\emptyset]$. The lattice Λ of invariant Laurent monomials consists of $u^i v^j$ with $\alpha i + j \equiv 0 \bmod r$; it is a lattice $\Lambda \cong \mathbb{Z}^2$, but with no preferred basis. The coordinate ring of S, based by $\mathbb{Z}/r$-invariant monomials, is minimally generated by monomials on the Newton boundary of the positive quadrant $\sigma \subset \Lambda_\mathbb{R}$. Setting $0 < \beta \leq r$ with $\alpha\beta = -1$ modulo r, these monomials are $x_0 = u^r$, $x_1 = u^\beta v$, etc. Either continued fraction $\frac{r}{\beta} = [a_1, \dots, a_{k-1}]$ or $\frac{r}{r-\alpha} = [a_{k-1}, \dots, a_1]$ provides the generators $x_{0 \dots k}$ and the *tag equations* holding between them:

$$x_{i-1} x_{i+1} = x_i^{a_i} \quad \text{for } i = 1, \dots, k-1. \tag{2.10}$$

In particular,

$$\begin{aligned} \frac{r}{\beta} &= [a_1, \dots, a_{k-1}] \quad \mapsto \quad x_0 = u^r,\ x_1 = u^\beta v,\ x_2 = x_1^{a_1} x_0^{-1}, \dots \\ \frac{r}{r-\alpha} &= [a_{k-1}, \dots, a_1] \quad \mapsto \quad x_k = v^r,\ x_{k-1} = uv^{r-\alpha}, \dots . \end{aligned} \tag{2.11}$$

The tag equations (2.10) determine S completely: they express any x_j as a Laurent monomial in any two consecutive monomials x_i, x_{i+1}. The complete intersection in $\mathbb{A}^{k+1}_{\langle x_{0\dots k}\rangle}$ given by (2.10) is S plus $\mathbb{A}^2_{\langle x_0, x_k\rangle}$ (usually with a nonreduced structure). The other generators of I_S are "long equations" $x_i x_j$ = monomial for $|i-j| > 2$, that can be deduced from (2.10) via syzygies.

2.2 Tents and fans

A *tent* $T = S_0 \cup S_1 \cup S_2 \cup S_3 \subset \mathbb{A}^{k+l+2}_{\langle x_{0\dots k}, y_{0\dots l}\rangle}$ is the union of the four affine toric surfaces of Figure 1.1, with horizontal sides $S_0 = \mathbb{A}^2_{\langle x_0, y_0\rangle}$ and $S_2 = \mathbb{A}^2_{\langle x_k, y_l\rangle}$ and vertical sides the cyclic quotient singularities

$$\begin{aligned} &S_1 = \tfrac{1}{r}(\alpha, 1) \text{ with coordinates } x_{k\dots 0} \text{ from } \tfrac{r}{r-\alpha} = [a_{k-1}, \dots, a_1], \text{ and} \\ &S_3 = \tfrac{1}{s}(\beta, 1) \text{ with coordinates } y_{l\dots 0} \text{ from } \tfrac{s}{s-\beta} = [b_{l-1}, \dots, b_1], \end{aligned}$$

where $\alpha \le r$ are coprime natural numbers, and similarly for $\beta \le s$ (there are no other conditions on α, β at this stage). The coordinates $x_{0\dots k}, y_{0\dots l}$ of the ambient space $\mathbb{A}^{k+l+2}$ and the equations for T are shown schematically in Figure 2.1; once we have added *corner tags* in 2.2.2 and *annotations* in 2.3, we refer to such arrays as *long rectangles*, and use them as a shorthand for certain toric 4-folds. The components glue transversally along their toric strata (= coordinate axes), giving T four singular axes of transverse ordinary double points; the two axes on S_2 are the *top* axes, and the two on S_0 the *bottom* axes.

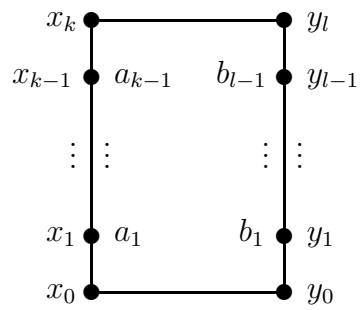

Figure 2.1: Coordinates and tags for a tent T

2.2.1 Tents without embeddings

Our definition expresses T embedded in $\mathbb{A}^{k+l+2}$ by explicit coordinates; its ideal I_T is generated by I_{S_1} and I_{S_3}, determined by the tags down the sides as in 2.1, together with the cross-equations $x_i y_j = 0$ for all pairs $(i,j) \neq (0,0), (k,l)$.

However, T can be viewed abstractly as an identification scheme as studied more generally in Reid [dP]: write $\Gamma'_i \cup \Gamma''_i$ for the toric 1-strata of the S_i and $C = \bigsqcup_{i=1}^4 (\Gamma'_i \cup \Gamma''_i)$. Let D be the four axes $\mathbb{A}^1$ with coordinates x_0, x_k, y_l, y_0 glued transversally at a common origin (as coordinate axes in $\mathbb{A}^4$); write $\varphi\colon C \to D$ for the morphism given by x_0 on the x_0-axes of S_0 and S_1, and so on, to perform the identifications of Figure 1.1. Then

$$T = \big(S_0 \sqcup S_1 \sqcup S_2 \sqcup S_3\big)/\varphi. \tag{2.12}$$

There are no parameters or moduli in this glueing.

Lemma 2.3 *Let T be the tent as above. Then T is a Gorenstein scheme. Moreover, T has an action of $(\mathbb{G}_m)^4$ that restricts to the toric structure on each component.*

Proof We use elementary results of [dP], Section 2. T is Cohen–Macaulay because all the glueing happens in codimension 1 ([dP], 2.2). We prove it is Gorenstein using the criterion of [dP], Corollary 2.8.

Each component S_i is a toric surface; on each, choose a $\mathbb{Z}$-basis m_1, m_2 for the monomial lattice, oriented clockwise (e.g., on S_1, take x_0, x_1 or x_{k-1}, x_k; on S_2, take x_k, y_l). The 2-form $s = \frac{\mathrm{d}\,m_1}{m_1} \wedge \frac{\mathrm{d}\,m_2}{m_2} \in \Omega^2_{\mathbb{T}}$ on the big torus is a basis for $\Omega^2_{\mathbb{T}}$, is defined over $\mathbb{Z}$, independent of the choice of oriented basis, and has log poles along each stratum of S, with residue along each stratum $\mathbb{A}^1$ equal to $\pm$ times the natural basis $\frac{\mathrm{d}\,m}{m}$ of $\Omega^1_{\mathbb{T}'}$. We take this basis element s on each component. Under the identification $\varphi\colon C \to D$ of the double locus, over the general point of each component of D, the residues from the two components are $\pm\frac{\mathrm{d}\,m}{m}$, and therefore cancel out; thus s satisfies the conditions of [dP], Corollary 2.8.ii and is a basis of the dualising sheaf ω_T.

Each component of T is a toric variety, so $(\mathbb{G}_m)^8$ acts on the disjoint union of the components. Each glueing imposes one linear condition on the action; we think of $\mathbb{T}_{S_0} = (\mathbb{G}_m)^2 = \{(\lambda_0, 1, 1, \lambda_3)\}$ as the big torus of S_0 and $\mathbb{T}_{S_1} = \{(\lambda_0, \lambda_1, 1, 1)\}$ that of S_1, etc. Q.E.D.

2.2.2 The fan $\Phi\left(\begin{smallmatrix} r & a \\ b & s \end{smallmatrix}\right)$ in the plane given by $\left(\begin{smallmatrix} r & a \\ b & s \end{smallmatrix}\right) \in \mathrm{SL}(2,\mathbb{Z})$

Jung–Hirzebruch continued fractions factor a base change in $\mathrm{SL}(2,\mathbb{Z})$ into elementary moves (Proposition 2.1(a)); in our case, the base change goes from the monomials x_0, y_0 at the bottom of our long rectangle to x_k, y_l at the top (up to sign and orientation). 2.3 constructs the toric variety V_{AB} and the first extension $T \subset V_{AB}$ generalising (1.7), using a matrix in $\mathrm{SL}(2,\mathbb{Z})$ to generate the monomial cone σ_{AB} of Figure 2.3 in the 4-dimensional lattice $\mathbb{M} = \mathbb{Z}^4$.

We start by analysing the combinatorics of this construction in a stripped-down 2-dimensional setting $\overline{\mathbb{M}} = \mathbb{Z}^2$. Consider two oriented bases x_0, y_0 and η, ξ of $\overline{\mathbb{M}}$ related by inverse base changes

$$x_0 = \eta^{-r}\xi^a, \quad y_0 = \eta^b\xi^{-s} \quad \text{and} \quad \eta = x_0^{-s}y_0^{-a}, \quad \xi = x_0^{-b}y_0^{-r}. \tag{2.13}$$

Here $r, s, a, b \geq 0$ are integers with $rs - ab = 1$, so

$$\begin{pmatrix} r & a \\ b & s \end{pmatrix} \quad \text{and} \quad \begin{pmatrix} s & -a \\ -b & r \end{pmatrix} \in \mathrm{SL}(2, \mathbb{Z}) \tag{2.14}$$

are a pair of inverse elements. (If a or $b = 0$ then $r = s = 1$, and one or two points in what follows need minor restatement. Rather than do that systematically, it is easier simply to list all these initial cases, as in 2.2.4.)

The vectors x_0, y_0, η, ξ subdivide the plane $\overline{\mathbb{M}}_{\mathbb{R}}$ into the fan $\Phi(\begin{smallmatrix} r & a \\ b & s \end{smallmatrix})$ of Figure 2.2.a consisting of 4 cones $\langle x_0, y_0\rangle$, $\langle x_0, \xi\rangle$, $\langle \xi, \eta\rangle$, $\langle y_0, \eta\rangle$. It determines a tent T, with coordinate ring generated by the 4 monomial cones and related by $m_1 m_2 = 0$ if m_1, m_2 are not in a common cone. The next lemma computes the affine toric surfaces that make up the tent T corresponding to $\Phi(\begin{smallmatrix} r & a \\ b & s \end{smallmatrix})$; compare with the first long rectangle of Example 1.2 for which $(\begin{smallmatrix} r & a \\ b & s \end{smallmatrix}) = (\begin{smallmatrix} 7 & 12 \\ 4 & 7 \end{smallmatrix})$.

Lemma 2.4 *Suppose that $r, s, a, b \geq 1$. Consider the cone $\langle x_0, \xi\rangle$ (marked S_1 in Figure 2.2(a)). The lattice $\overline{\mathbb{M}}$ is generated by the monomials x_0, ξ together with either of*

$$y_0^{-1} = (x_0^b\xi)^{1/r} \quad \textit{or} \quad \eta = (x_0^{-1}\xi^a)^{1/r}.$$

Therefore $\langle x_0, \xi\rangle$ is the monomial cone $\frac{1}{r}(\alpha, 1)$ or $\frac{1}{r}(1, r - \beta)$, where α is the least residue of a mod r, and β that of b (note that $rs - ab = 1$ implies α and $r - \beta$ are inverse mod r).

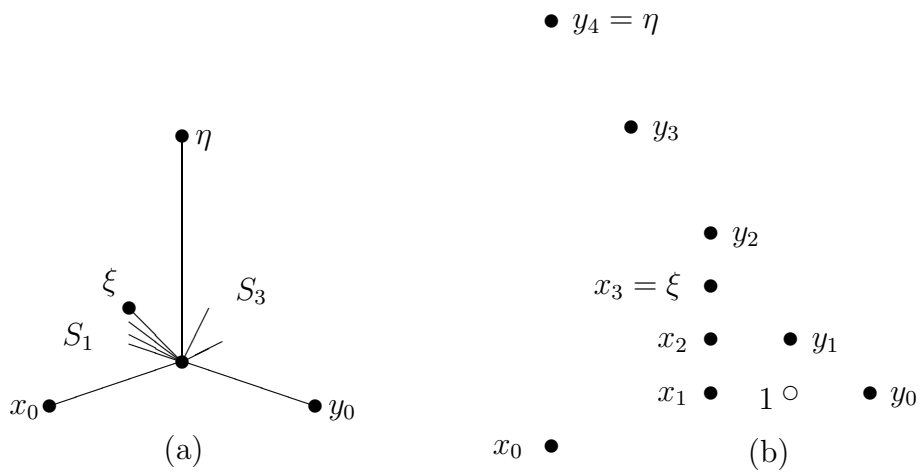

Figure 2.2: The fan $\Phi(\begin{smallmatrix} r & a \\ b & s \end{smallmatrix}) \in \mathrm{SL}(2, \mathbb{Z})$ defined by x_0, y_0, η, ξ

Write $x_0, x_1, \dots, x_{k-1}, x_k = \xi$ for the successive monomials along the Newton boundary of $\langle x_0, \xi\rangle$. The number k and the monomials themselves come from factoring the base change (2.13) *into elementary moves:*

$$\begin{pmatrix} -r & a \\ b & -s \end{pmatrix} = \begin{pmatrix} 0 & 1 \\ -1 & a_0 \end{pmatrix} \begin{pmatrix} 0 & 1 \\ -1 & a_1 \end{pmatrix} \cdots \begin{pmatrix} 0 & 1 \\ -1 & a_{k-1} \end{pmatrix} \begin{pmatrix} 0 & 1 \\ -1 & a_k \end{pmatrix}, \tag{2.15}$$

in which each of $a_1, \dots, a_{k-1} \geq 2$. More concretely, they are given by the continued fraction expansions

$$[a_0, a_1, \dots, a_{k-1}] = \frac{-b}{r} \quad \textit{and} \quad [a_k, \dots, a_1] = \frac{a}{r} \tag{2.16}$$

by either of the following constructions:

(1) From the bottom, x_0 is given, and $x_1 = (x_0^\beta \xi)^{1/r}$, where β is the least residue of b mod r*. Thus $a_0 = \lceil \frac{-b}{r} \rceil = \frac{-b+\beta}{r} \leq 0$ and*

$$x_1 = (x_0^\beta \xi)^{1/r} = y_0^{-1} x_0^{a_0}, \quad \textit{that is,} \quad x_1 y_0 = x_0^{a_0}. \tag{2.17}$$

If $\beta = 0$ then r divides b, whereas $rs - ab = 1$ implies that r, b are coprime; thus $r = 1$, so that $k = 1$ and $x_1 = \xi$. Otherwise $x_2, \dots, x_k$ are determined as usual by tag equations

$$x_{i-1} x_{i+1} = x_i^{a_i} \quad \textit{for } i = 1, \dots, k-1,$$

where $[a_1, \dots, a_{k-1}] = \frac{r}{\beta}$ (see Remark 2.2).

(2) From the top, $x_k = \xi$ is given; if $r \mid a$ then, as before, $r = 1$ and the only monomials are $x_0, x_1 = \xi$. Otherwise, set $x_{k-1} = (x_0 \xi^{r-\alpha})^{1/r}$, where α is the least residue of a mod r*. Then $r - \alpha = a_k r - a$ where $a_k = \lceil \frac{a}{r} \rceil \geq 1$, and*

$$x_{k-1} = \xi^{a_k} (x_0 \xi^{-a})^{1/r} = x_k^{a_k} \eta^{-1} \quad \textit{that is,} \quad x_{k-1} \eta = x_k^{a_k}.$$

The remaining monomials are determined by

$$x_{i-1} x_{i+1} = x_i^{a_i}, \quad \textit{where } [a_{k-1}, \dots, a_1] = \tfrac{r}{r-\alpha}.$$

In the same way, the sequence $[b_0, b_1, \dots, b_l]$ factors the inverse transformation of (2.13) *into elementary moves:*

$$\begin{pmatrix} -s & -a \\ -b & -r \end{pmatrix} = \begin{pmatrix} 0 & 1 \\ -1 & b_l \end{pmatrix} \begin{pmatrix} 0 & 1 \\ -1 & b_{l-1} \end{pmatrix} \cdots \begin{pmatrix} 0 & 1 \\ -1 & b_1 \end{pmatrix} \begin{pmatrix} 0 & 1 \\ -1 & b_0 \end{pmatrix}. \tag{2.18}$$

More concretely, $\langle y_0, \eta\rangle$ is the monomial cone $\frac{1}{s}(b, 1)$ or $\frac{1}{s}(1, -a)$, and the tags and monomials on the S_3 side are $b_0, \dots, b_l$ and $y_0, \dots, y_k$, given by

$$[b_0, b_1, \dots, b_{l-1}] = \frac{-a}{s} \quad \textit{and} \quad [b_l, \dots, b_1] = \frac{b}{s} \tag{2.19}$$

and $y_1 = x_0^{-1} y^{b_0} = (y_0^\beta \eta)^{1/s}$ where β is the least residue of b mod s*.*

Not every tent $T = S_0 \cup S_1 \cup S_2 \cup S_3$ is given by a fan $\Phi(\begin{smallmatrix} r & a \\ b & s \end{smallmatrix})$. Which are? And in how many ways? What extra data does the fan know about beyond T? The tent T knows the 4 monomial cones up to $\mathrm{SL}(2,\mathbb{Z})$ isomorphism, but does not know how they fit together in $\mathbb{Z}^2$; it knows the fractions $\frac{1}{r}(\alpha,1)$ and $\frac{1}{s}(\beta,1)$, but not the corner tags a_0, b_0, a_k, b_l.

Corollary 2.5 *The fan $\Phi(\begin{smallmatrix} r & a \\ b & s \end{smallmatrix})$ gives T with $S_1 = \frac{1}{r}(\alpha,1)$, $S_3 = \frac{1}{s}(\beta,1)$ by the construction of 2.2.2 if and only if $a \equiv \alpha \bmod r$ and $b \equiv \beta \bmod s$.*

For fixed T, except for initial cases with $r = s = 1$ (see 2.2.4), there are 0, 1 or 2 matrixes for which $\Phi(\begin{smallmatrix} r & a \\ b & s \end{smallmatrix})$ gives T:

- *if neither α nor β divides $rs-1$, there are none;*
- *if α divides $rs-1$ then $a = \alpha$, $b = (rs-1)/\alpha$ provides a solution;*
- *similarly, if $\beta \mid (rs-1)$ then $a = (rs-1)/\beta$, $b = \beta$ provides a solution.*

Remark 2.6 Whereas Figure 2.2(a) sketches the division of the plane into 4 cones $\langle x_0, y_0\rangle$, $\langle x_0, \xi\rangle$, $\langle \xi, \eta\rangle$, $\langle y_0, \eta\rangle$, 2.2(b) accurately plots the monomials in the case $(\begin{smallmatrix} r & a \\ b & s \end{smallmatrix}) = (\begin{smallmatrix} 7 & 24 \\ 2 & 7 \end{smallmatrix})$, with tags $[a_0, \dots, a_3] = [0, 4, 2, 4]$ at the x_i and $[b_0, \dots, b_4] = [-3, 3, 2, 2, 1]$ at the y_i. The comparison of the rich and messy reality of 2.2(b) with our square-cut projective pictures such as Figures 1.2–1.3 and 2.1 is startling but enlightening: it reveals, for example,

$$\begin{aligned} a_0 = 0 \text{ at } x_0 &\implies x_1, 0, y_0 \text{ are in arithmetic progression;} \\ b_4 = 1 \text{ at } y_4 &\implies 0 x_3 y_4 y_3 \text{ is a parallelogram;} \\ b_0 = -3 \text{ at } y_0 &\implies 1 \text{ is in the affine convex hull } 1 \in \langle x_0, y_1, y_0\rangle, \end{aligned}$$

and so on. The figure and its monomials have other convexity and collinearity properties to which we return later (compare the Scissors of Figure 4.2).

2.2.3 Big end, little end, and attitude of a long rectangle

In the $\mathrm{SL}(2,\mathbb{Z})$ geometry of the plane, all basic cones are equivalent, so there is of course no notion of the *size* of an angle. Despite this, the bottom cone $\langle x_0, y_0\rangle$ is clearly the *big end* of the fan Φ in Figure 2.2: if we view Φ as a pie chart, $\langle x_0, y_0\rangle$ occupies the lion's share of the plane, practically 50%. The issue is not size, but convexity. Our choice of signs in (2.13) is equivalent to

$$-\langle \xi, \eta\rangle \subseteq \langle x_0, y_0\rangle\,. \tag{2.20}$$

Even more holds: every monomial appearing as a minimal generator in the other cones has inverse in $\langle x_0, y_0\rangle$.

Our choices in Φ have already decided that the bottom $S_0 = \mathbb{A}^2_{\langle x_0, y_0\rangle}$ is its big end and the top $S_2 = \mathbb{A}^2_{\langle \xi, \eta\rangle}$ its little end. (The two players will swap ends for the second half of the game.) Once this choice is out of the way, there are still two dichotomies for the corner tags, forming a division into 4 cases, the *attitude* of the long rectangle and of the panel V_{AB}. Treating this carefully here will save many headaches later.

Corollary 2.7 *Except for initial cases with r or $s = 1$ (see 2.2.4) $r, s \neq a, b$ and*

$$r < a \iff b < s \quad \textit{and} \quad r < b \iff a < s.$$

The long rectangle σ_{AB} thus has attitude:

Top tags: *either* $a_k \geq 2$ *and* $b_l = 1$ *if* $r < a$ *and* $b < s$*; or*
$a_k = 1$ *and* $b_l \geq 2$ *if* $r > a$ *and* $b > s$*; and*

Bottom tags: *either* $a_0 \leq -1$ *and* $b_0 = 0$ *if* $r < b$ *and* $a < s$*; or*
$a_0 = 0$ *and* $b_0 \leq -1$ *if* $r > b$ *and* $a > s$*.*

Corollary 2.8 *If $a_0 < 0$ and $b_0 = 0$ then $[a_2, \ldots, a_k, b_l, \ldots, b_2, b_1] = 0$. If $a_0 = 0$ and $b_0 < 0$ then $[a_1, \ldots, a_k, b_l, \ldots, b_2] = 0$.*

Conversely, given $\frac{1}{r}(\alpha, 1)$ and $\frac{1}{s}(\beta, 1)$, the tent T is given by a fan $\Phi(\begin{smallmatrix} r & a \\ b & s \end{smallmatrix})$ with big end $S_0 = \mathbb{A}^2_{\langle x_0, y_0 \rangle}$ if and only if the continued fractions

$$\frac{r}{r - \alpha} = [a_{k-1}, \ldots, a_1] \quad \textit{and} \quad \frac{s}{s - \beta} = [b_{l-1}, \ldots, b_1]$$

can be concatenated with a_k and b_l such that

$$\textit{either} \quad [a_2, \ldots, a_k, b_l, \ldots, b_2, b_1] = 0 \quad \textit{or} \quad [a_1, a_2 \ldots, a_k, b_l, \ldots, b_2] = 0.$$

Proof x_1 and y_0 are opposite vectors in Figure 2.2, so $\langle x_1, x_2, \ldots, y_1, y_0 \rangle$ is a half-space with a basic subdivision. Q.E.D.

2.2.4 Initial cases

We list here all the cases with r or $s \leq 1$, treating all cases with attitude not covered by Corollary 2.7.

$\begin{pmatrix} 1 & 0 \\ 0 & 1 \end{pmatrix}$	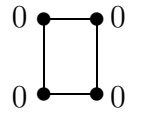	$x_0y_1 = A,$ $x_1y_0 = B.$
$\begin{pmatrix} 1 & 0 \\ b & 1 \end{pmatrix}$	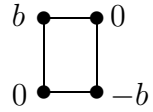	$x_0y_1 = x_1^bA,$ $x_1y_0 = B.$
$\begin{pmatrix} 1 & a \\ 0 & 1 \end{pmatrix}$	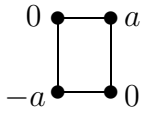	$x_0y_1 = A,$ $x_1y_0 = y_1^aB.$
$\begin{pmatrix} 1 & 1 \\ s-1 & s \end{pmatrix}$	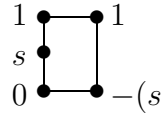	$x_1y_1 = x_2A, x_2y_0 = y_1B,$ $x_0x_2 = x_1^s,$ $x_1y_0 = AB, x_0y_1 = x_1^{s-1}A.$
$\begin{pmatrix} r & 1 \\ r-1 & 1 \end{pmatrix}$	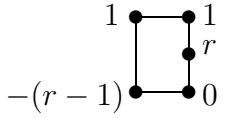	$x_0y_1 = x_2A, x_1y_1 = y_1B,$ $y_0y_2 = y_1^r,$ $x_1y_0 = y_1^{r-1}B, x_0y_1 = AB.$

The cases with a or $b = 1$ and $r, s \geq 2$ are not exceptional; rather, they serve as the first regular example of our construction:

$$\begin{pmatrix} r & rs-1 \\ 1 & s \end{pmatrix} \quad \text{ 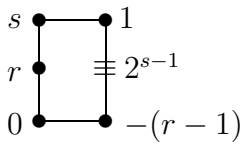 } \quad \begin{pmatrix} r & 1 \\ rs-1 & s \end{pmatrix} \quad \text{ 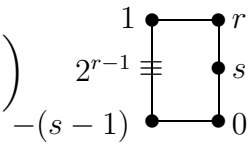 } \tag{2.21}$$

2.3 Construction of $T \subset V_{AB}$ from $\left(\begin{smallmatrix} r & a \\ b & s \end{smallmatrix}\right) \in \mathrm{SL}(2, \mathbb{Z})$

To construct the deformation $T \subset V_{AB}$, we pump up the fan $\Phi(\left(\begin{smallmatrix} r & a \\ b & s \end{smallmatrix}\right)$ of 2.2.2 out of the plane $\overline{\mathbb{M}}$ to the cone σ_{AB} of Figure 2.3 in the 4-space of $\mathbb{M} = \mathbb{Z}^4$, using the new variables A, B respectively to bend along the ξ and η axes. In more detail, consider the monomial lattice $\mathbb{M} \cong \mathbb{Z}^4$ based by ξ, η, A, B, and the cone σ_{AB} in $\mathbb{M}_{\mathbb{R}}$ spanned by

$$\xi, \eta, A, B \quad \text{together with} \quad x_0 = (A\eta^{-1})^r\xi^a, \quad y_0 = \eta^b(B\xi^{-1})^s \tag{2.22}$$

(compare these with the equations of (2.13)). We draw σ_{AB} projectively, so that it has two quadrilateral faces $\xi\eta Ax_0$ and $\xi\eta y_0B$ (the "back"), and four triangles ξBx_0, Bx_0y_0, x_0y_0A and $y_0A\eta$ (the "front"). The primitive vectors orthogonal to these faces are, in order,

$$(0,0,0,1)\ \ (0,0,1,0)\ \ (0,1,1,0)\ \ (rb, rs, 1, 0)\ \ (rs, as, 0, 1)\ \ (1,0,0,1). \tag{2.23}$$

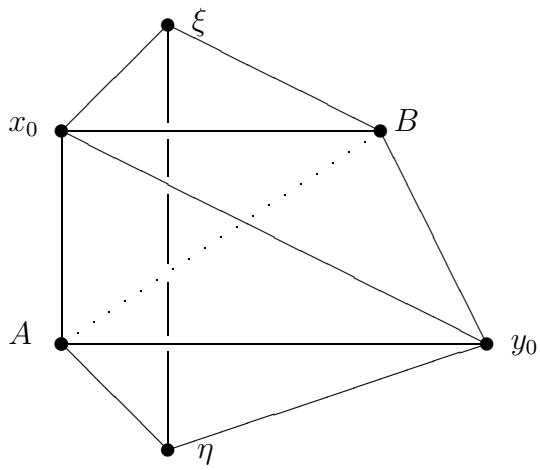

Figure 2.3: The monomial cone σ_{AB}

We get σ_{AB} from the simplex $\langle \xi, \eta, x_0, y_0 \rangle$ by pulling out each of the two back faces to quadrilaterals, adding a vertex A in the plane of x_0, ξ, η such that ξ, η, A is basic and the quadrilateral x_0, ξ, η, A is convex as shown, and likewise for B in the plane of y_0, η, ξ. The picture can be viewed from different perspectives (we use some below, see Figure 4.1), and trying to read metric properties from these can be misleading.

The dual cone $\sigma_{AB}^\vee$ is the convex hull of the orthogonal vectors (2.23). Since these are all in the hyperplane of weights w with $w(AB) = 1$, the dotted line from A to B is interior to σ_{AB}, and AB generates the ideal of interior monomials. This is Danilov's criterion for the toric variety $V_{AB} = \mathrm{Spec}(\mathbb{C}[\sigma_{AB} \cap \mathbb{M}])$ to be Gorenstein. The unextended simplex $\langle \xi, \eta, x_0, y_0 \rangle$ itself does not in general determine A, B or the matrixes (2.14).

The 2-faces $\langle x_0, \xi \rangle$ and $\langle y_0, \eta \rangle$ of the simplicial cone $\langle \xi, \eta, x_0, y_0 \rangle$ are also faces of σ_{AB}, basic in $\mathbb{M}$ if and only if $r = 1$, respectively $s = 1$; they are the monomial cones of toric surfaces S_1 and S_3, and are determined exactly as in 2.2.2. The new feature is the relations (2.22) and their inverses

$$\eta = (A^r B^a x_0^{-1})^s y_0^{-a}, \quad \xi = x_0^{-b}(A^b B^s y_0^{-1})^r \tag{2.24}$$

that determine tag relations at the corners. Indeed (2.22) and (2.24) give

$$\begin{matrix} (x_0 \xi^{-a})^{1/r} = A\eta^{-1} & \text{and} & (y_0 \eta^{-b})^{1/s} = B\xi^{-1} \\ (x_0^b \xi)^{1/r} = A^b B^s y_0^{-1} & \text{and} & (y_0^a \eta)^{1/s} = A^r B^a x_0^{-1} \end{matrix} \in M. \tag{2.25}$$

and the analogue of Lemma 2.4 follows as in 2.2.2.

Lemma 2.9 *The face $\langle x_0, \xi \rangle$ spans a 2-dimensional vector space in $\mathbb{M}_\mathbb{R}$, that intersects $\mathbb{M}$ in the sublattice generated as a $\mathbb{Z}$-module by x_0, ξ together with* either *of*

$$(x_0^b \xi)^{1/r} = A^b B^s y_0^{-1} \quad \textit{or} \quad (x_0 \xi^{-a})^{1/r} = A\eta^{-1}.$$

Write $x_0, x_1, \ldots, x_{k-1}, x_k = \xi$ for the successive monomials along the Newton boundary of $\langle x_0, \xi\rangle$. The number k and the monomials themselves come from either of the continued fraction expansions

$$[a_0, a_1, \ldots, a_{k-1}] = \frac{-b}{r} \quad \text{and} \quad [a_k, \ldots, a_1] = \frac{a}{r} \tag{2.26}$$

by the following constructions:

1. *From the bottom, x_0 is given, and $x_1 = (x_0^\beta \xi)^{1/r}$, where β is the least residue of b modulo r. Thus $a_0 = \lceil \frac{-b}{r} \rceil = \frac{-b+\beta}{r} \le 0$ and*

$$x_1 = (x_0^\beta \xi)^{1/r} = A^b B^s x_0^{a_0} y_0^{-1}, \quad \text{that is,} \quad x_1 y_0 = A^b B^s x_0^{a_0}. \tag{2.27}$$

   If $\beta = 0$ then r divides b, whereas $rs - ab = 1$ implies that r, b are coprime; thus $r = 1$, so that $k = 1$ and $x_1 = \xi$. Otherwise $x_2, \ldots, x_k$ are determined as usual by tag equations

$$x_{i-1}x_{i+1} = x_i^{a_i} \quad \text{for } i = 1, \ldots, k-1,$$

   where $[a_1, \ldots, a_{k-1}] = \frac{r}{\beta}$ (see Remark 2.2).

2. *From the top, $x_k = \xi$ is given; if $r \mid a$ then, as before, $r = 1$ and the only monomials are $x_0, x_1 = \xi$. Otherwise, set $x_{k-1} = (x_0 \xi^{r-\alpha})^{1/r}$, where α is the least residue of a mod r. Then $r - \alpha = a_k r - a$ where $a_k = \lceil \frac{a}{r} \rceil \ge 1$, and*

$$x_{k-1} = \xi^{a_k}(x_0 \xi^{-a})^{1/r} = x_k^{a_k} A \eta^{-1} \quad \text{that is,} \quad x_{k-1}\eta = A x_k^{a_k}.$$

   The remaining monomials are determined by

$$x_{i-1}x_{i+1} = x_i^{a_i}, \quad \text{where } [a_{k-1}, \ldots, a_1] = \tfrac{r}{r-\alpha}.$$

The ring $\mathbb{C}[\mathbb{M} \cap \langle x_0, \xi\rangle] = \mathbb{C}[S_1]$ is isomorphic to the invariant ring of the cyclic quotient singularity $\frac{1}{r}(a, 1) \cong \frac{1}{r}(1, -b)$; here $ab = rs - 1$, so that $ab \equiv -1 \bmod s$.

In the same way, $\langle y_0, \eta\rangle \cong \frac{1}{s}(b, 1) \cong \frac{1}{s}(1, -a)$ with initial monomials y_1 and y_{l-1} determined by the corner tag equations

$$x_0 y_1 = A^r B^a y_0^{b_0} \quad \text{and} \quad \xi y_{l-1} = B \eta^{b_l},$$

with $b_0 = \lceil \frac{-a}{s} \rceil \le 0$ and $b_l = \lceil \frac{b}{s} \rceil \ge 1$, and the remaining monomials for S_3 are $y_0, y_1, \ldots, y_{l-1}, y_l$ tagged by

$$[b_0, b_1, \ldots, b_{l-1}] = \frac{-a}{s} \quad \text{and} \quad [b_l, \ldots, b_1] = \frac{b}{s}. \tag{2.28}$$

In conclusion, the following theorem states the complete solution to toric deformation of tents that smooth the axes at one end.

Theorem 2.10 *Let*

$$T = S_0 \cup S_1 \cup S_2 \cup S_3$$

be a tent with two given cyclic quotient singularities in reduced form $S_1 = \frac{1}{r}(\alpha, 1)$ *and* $S_3 = \frac{1}{s}(\beta, 1)$. *Then toric deformations* $T \subset V_{AB}$ *that smooth the* ξ *and* η *axes correspond one-to-one with matrixes*

$$\begin{pmatrix} r & a \\ b & s \end{pmatrix} \in \mathrm{SL}(2, \mathbb{Z}) \quad \textit{with} \quad \begin{array}{l} a \equiv \alpha \bmod r, \\ b \equiv \beta \bmod s. \end{array}$$

Since $ab = rs - 1$ *obviously implies that* $a < r$ *or* $b < s$, *this means that*

$$\begin{array}{rl} \textit{either} & a = \alpha \mid rs - 1 \quad \textit{and} \quad b = \frac{rs-1}{\alpha}\,, \\ \textit{or} & b = \beta \mid rs - 1 \quad \textit{and} \quad a = \frac{rs-1}{\beta}\,. \end{array}$$

There may be 0, 1 *or* 2 *solutions.*

3 Classification of diptychs

A *diptych*, for a tent T, is a pair of toric deformations

$$T \subset V_{AB} \quad \text{and} \quad T \subset V_{LM}$$

(the two *panels* of the diptych), in which the first smooths the top axes and the second smooths the bottom axes.

Our construction in 2.3 of $T \subset V_{AB}$ is given, already at the level of T, by the fan $\Phi(\begin{smallmatrix} r & a \\ b & s \end{smallmatrix})$ dividing the plane $\overline{\mathbb{M}}$ into the four cones of Figure 2.2. Its key properties are that its four cones give the four sides of T, and the union of its three top cones is *one step beyond convex*; by this we mean that shaving either x_0 or y_0 off the two side cones makes the union of the three top cones convex, which we express by saying that the cone $\langle x_0, y_0 \rangle$ corresponding to S_0 is the *big end* of the fan.

3.1 A second fan $\Phi'(\begin{smallmatrix} r & g \\ h & s \end{smallmatrix})$ and a second panel V_{LM}

For the right panel V_{LM} of our diptych, we need a second fan Φ' in a plane $\overline{\mathbb{M}}'$ (not identified with $\overline{\mathbb{M}}$), defining the same tent T, but this time the big end of Φ' is the top $\langle \xi, \eta \rangle$ corresponding to S_2, and its little end the bottom $\langle x_0, y_0 \rangle$ corresponding to S_0. For this, replace (2.13) with the base change

$$x_0 = \eta^{-r}\xi^{-g}, \quad y_0 = \eta^{-h}\xi^{-s} \quad \text{and} \quad \eta = x_0^{-s}y_0^{g}, \quad \xi = x_0^{h}y_0^{-r} \tag{3.1}$$

based on the inverse pair $(\begin{smallmatrix} -r & -g \\ -h & -s \end{smallmatrix})$ and $(\begin{smallmatrix} -s & g \\ h & -r \end{smallmatrix})$, with $g, h \geq 0$. As before, x_0, ξ, η, y_0 define a fan Φ' of 4 cones, but with signs giving the inclusion $-\langle x_0, y_0 \rangle \subseteq \langle \xi, \eta \rangle$ opposite to (2.20), so that $\langle \xi, \eta \rangle$ is the big end.

Lemma 3.1 *In Φ' the cone $\langle x_0, \xi\rangle$ corresponding is $\frac{1}{r}(1,h) \cong \frac{1}{r}(-g,1)$; the cone $\langle y_0, \eta\rangle$ is $\frac{1}{s}(1,g) \cong \frac{1}{s}(-h,1)$.*

Hence Φ' defines the same tent T as Φ of 2.2.2 if and only if $-g \equiv \alpha \bmod r$ and $-h \equiv \beta \bmod s$.

We say that Φ and Φ' related in this way are *partners*. 3.2 classifies all partner pairs. The analysis of the coordinate ring of V_{AB} in Lemma 2.9 can be applied, with the ends exchanged, to V_{LM} to prove immediately:

Lemma 3.2 *From V_{AB}, the cone $\langle x_0, \xi\rangle$ is $\frac{1}{r}(a,1) \cong \frac{1}{r}(1,-b)$ and from V_{LM} it is $\frac{1}{r}(1,g) \cong \frac{1}{r}(-h,1)$. The cone $\langle y_0, \eta\rangle$ is $\frac{1}{s}(b,1) \cong \frac{1}{s}(1,-a)$ and also $\frac{1}{s}(1,h) \cong \frac{1}{s}(-g,1)$. Therefore $ag \equiv 1 \bmod r$ and $bh \equiv 1 \bmod s$; together with $rs - ab = rs - gh = 1$, these imply that*

$$a + h \equiv b + g \equiv 0 \bmod r \text{ and } \bmod s. \tag{3.2}$$

We draw the two monomial cones σ_{AB} and σ_{LM} together in Figure 4.1; it is easy to see that the union $\sigma_{AB} \cup \sigma_{LM}$ has convex hull a cone with a vertex.

As an example and sanity check, it is a fun exercise to run through $\left(\begin{smallmatrix} r & a \\ b & s \end{smallmatrix}\right) = \left(\begin{smallmatrix} 7 & 12 \\ 4 & 7 \end{smallmatrix}\right)$ and $\left(\begin{smallmatrix} r & g \\ h & s \end{smallmatrix}\right) = \left(\begin{smallmatrix} 7 & 24 \\ 2 & 7 \end{smallmatrix}\right)$ to recover the two long rectangles of Example 1.2.

3.2 Classification of partner pairs

Classifying all partner pairs Φ, Φ' of fans is an elementary "infinite descent".

Rules of the game: Given integers

$$\begin{gathered} r, s \geq 1, \quad a, b, g, h \geq 0, \quad \text{with} \quad ab = gh = rs - 1 \\ \text{and} \quad a + h \equiv b + g \equiv 0 \bmod r \text{ and } \bmod s. \end{gathered} \tag{3.3}$$

Use the congruences to define two integers $d \geq 1$ and $e \geq 1$:

$$a + h = ds \quad \text{and} \quad b + g = er. \tag{3.4}$$

Theorem 3.3 (Classification Theorem I) *Each solution of (3.3–3.4) is one of the exceptional solutions* (3.8) *below, or is given either by*

$$\begin{aligned} \begin{pmatrix} r & a \\ b & s \end{pmatrix} &= \begin{pmatrix} d & -1 \\ 1 & 0 \end{pmatrix} \begin{pmatrix} e & -1 \\ 1 & 0 \end{pmatrix} \cdots \begin{pmatrix} e \text{ or } d & -1 \\ 1 & 0 \end{pmatrix} \begin{pmatrix} 0 & 1 \\ -1 & 0 \end{pmatrix}, \\ \begin{pmatrix} r & g \\ h & s \end{pmatrix} &= \begin{pmatrix} 0 & 1 \\ -1 & 0 \end{pmatrix} \begin{pmatrix} 0 & -1 \\ 1 & d \text{ or } e \end{pmatrix} \cdots \begin{pmatrix} 0 & -1 \\ 1 & d \end{pmatrix} \begin{pmatrix} 0 & -1 \\ 1 & e \end{pmatrix} \end{aligned} \tag{3.5}$$

or the same with the two lefthand sides exchanged, or by

$$\begin{aligned} \begin{pmatrix} r & a \\ b & s \end{pmatrix} &= \begin{pmatrix} 0 & 1 \\ -1 & d \end{pmatrix} \begin{pmatrix} 0 & 1 \\ -1 & e \end{pmatrix} \cdots \begin{pmatrix} 0 & 1 \\ -1 & e \text{ or } d \end{pmatrix} \begin{pmatrix} 0 & -1 \\ 1 & 0 \end{pmatrix}, \\ \begin{pmatrix} r & g \\ h & s \end{pmatrix} &= \begin{pmatrix} 0 & -1 \\ 1 & 0 \end{pmatrix} \begin{pmatrix} d \text{ or } e & 1 \\ -1 & 0 \end{pmatrix} \cdots \begin{pmatrix} d & 1 \\ -1 & 0 \end{pmatrix} \begin{pmatrix} e & 1 \\ -1 & 0 \end{pmatrix} \end{aligned} \tag{3.6}$$

or the same with the two lefthand sides exchanged.

In each case, the values $d, e \geq 1$ alternate, the two lines have the same number $k+1$ of factors for some $k \geq 1$, and the values of d, e and k that are allowed are constrained only by the following table:

de	0	1	2	3	≥ 4
k	1	≤ 2	≤ 3	≤ 5	any

(3.7)

Exceptional solutions *The cases $b = g = 0$ or $a = h = 0$, the matrixes*

$$\begin{pmatrix} r & a \\ b & s \end{pmatrix} = \begin{pmatrix} 1 & a \\ 0 & 1 \end{pmatrix} \quad \text{and} \quad \begin{pmatrix} r & g \\ h & s \end{pmatrix} = \begin{pmatrix} 1 & 0 \\ h & 1 \end{pmatrix}, \tag{3.8}$$

for any $a, g \geq 0$, or the same with both matrixes transposed.

Remark 3.4 (1) In the statement, exchanging the two lefthand sides amounts to exchanging the roles of the two long rectangles, so exchanges V_{AB} and V_{LM} in the diptych (and turns them upside down if one draws them as long rectangles). Whether the first or second factorisation occurs depends on the attitude of the long rectangles, which is determined by whether $b < r$ or $b > r$; this becomes clear in the proof.

(2) The computation of a pair of long rectangles from these two matrices is implicit from Lemma 2.4, but we spell it out. The tags on the long rectangle of V_{AB} are given by the tags of the continued fraction expansion

$$-b/r = [a_0, \dots, a_{k-1}] \quad \text{and} \quad a/r = [a_k, \dots, a_1].$$

If $b < r$ and $d, e \geq 2$, then the alternating d, e tags run up the lefthand side, and the first of these will be of the form $[0, d, e, d, \dots]$. If either $d = 1$ or $e = 1$, the tags one computes are those after blowdown of the 1s, as in Proposition 2.1(b); one can reintroduce them by blowup as redundant generators to see the alternating d, e sequence. The tags down the righthand side are

$$-a/s = [b_0, \dots, b_{l-1}] \quad \text{and} \quad b/s = [b_l, \dots, b_1].$$

The tags on the long rectangle for V_{LM} are

$$g/r = [a'_0, a_1, \dots, a_{k-1}], \qquad -h/r = [a'_k, a_{k-1}, \dots, a_1]$$

and

$$h/s = [b'_0, b_1, \dots, b_{l-1}] \qquad -g/s = [b'_l, b_{l-1}, \dots, b_1]$$

where all but the corner tags are of course common to both long rectangles.

(3) The exceptional cases correspond to the not-very-long rectangles and not-very-surprising diptych varieties:

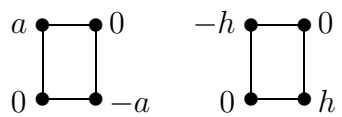

$$x_0 y_1 = A x_1^a + M y_0^h$$
$$x_1 y_0 = B + L$$

and we do not mention them again.

(4) The cases $b = h = 0$ or $a = g = 0$ are regular solutions in Theorem 3.3 with $k = 1$ and (say) $d = a$, $e = g$:

$$\begin{pmatrix} 1 & a \\ 0 & 1 \end{pmatrix} = \begin{pmatrix} d & -1 \\ 1 & 0 \end{pmatrix} \begin{pmatrix} 0 & 1 \\ -1 & 0 \end{pmatrix}, \quad \begin{pmatrix} 1 & g \\ 0 & 1 \end{pmatrix} = \begin{pmatrix} 0 & 1 \\ -1 & 0 \end{pmatrix} \begin{pmatrix} 0 & -1 \\ 1 & e \end{pmatrix}. \tag{3.9}$$

They provide the endpoint of our infinite descent:

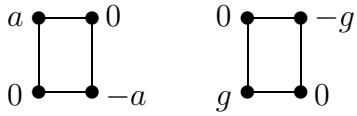

$$x_0 y_1 = A x_1^a + M$$
$$x_1 y_0 = B + L x_0^g$$

The equations can be used to eliminate variables B and M, so the diptych varieties in these cases are simply isomorphic to $\mathbb{C}^6$.

(5) The restriction on k when $de \leq 3$ in (3.7) arises because the product in (3.6) no longer satisfies $r, s, a, b \geq 0$ for bigger values of k. Thus

$$\begin{pmatrix} d & -1 \\ 1 & 0 \end{pmatrix} \begin{pmatrix} e & -1 \\ 1 & 0 \end{pmatrix} \begin{pmatrix} 0 & 1 \\ -1 & 0 \end{pmatrix} = \begin{pmatrix} d & de-1 \\ 1 & e \end{pmatrix}$$

has top righthand entry < 0 for $de = 0$ and $k = 2$. For $de = 1, 2, 3$ and $k = 3, 4, 6$ respectively, the product of k factors is -1:

$$\begin{pmatrix} d & -1 \\ 1 & 0 \end{pmatrix} \begin{pmatrix} e & -1 \\ 1 & 0 \end{pmatrix} \cdots \begin{pmatrix} d \text{ or } e & -1 \\ 1 & 0 \end{pmatrix} = \begin{pmatrix} -1 & 0 \\ 0 & -1 \end{pmatrix},$$

so we are basically into elements of finite order in $\mathrm{SL}(2, \mathbb{Z})$.

Proof of the Classification Theorem The following two operations preserve all the equalities and congruences in the rules of the game while interchanging the roles of e and d:

$$\begin{aligned} \begin{pmatrix} r & a \\ b & s \end{pmatrix} &\mapsto \begin{pmatrix} 0 & 1 \\ -1 & d \end{pmatrix} \begin{pmatrix} r & a \\ b & s \end{pmatrix} = \begin{pmatrix} b & s \\ db-r & h \end{pmatrix} \\ \begin{pmatrix} r & g \\ h & s \end{pmatrix} &\mapsto \begin{pmatrix} r & g \\ h & s \end{pmatrix} \begin{pmatrix} e & 1 \\ -1 & 0 \end{pmatrix} = \begin{pmatrix} b & r \\ eh-s & h \end{pmatrix} \end{aligned} \tag{3.10}$$

and ("its inverse with d, e interchanged")

$$\begin{aligned} \begin{pmatrix} r & a \\ b & s \end{pmatrix} &\mapsto \begin{pmatrix} e & -1 \\ 1 & 0 \end{pmatrix} \begin{pmatrix} r & a \\ b & s \end{pmatrix} = \begin{pmatrix} g & ea-s \\ r & a \end{pmatrix} \\ \begin{pmatrix} r & g \\ h & s \end{pmatrix} &\mapsto \begin{pmatrix} r & g \\ h & s \end{pmatrix} \begin{pmatrix} 0 & -1 \\ 1 & d \end{pmatrix} = \begin{pmatrix} g & dg-r \\ s & a \end{pmatrix} \end{aligned} \tag{3.11}$$

Indeed, under operation (3.10) transforms the equalities for the sums of opposing off-diagonal terms $a + h = ds$ and $b + g = er$ into

$$s + (eh - s) = eh \quad \text{and} \quad (db - r) + r = db.$$

The inequalities in the rules of the game need not be preserved, but their failure is a termination condition.

It turns out that a series of these operations (say using (3.10) to result in (3.5)) with alternating e, d reduces to the *initial case* $\left(\begin{smallmatrix} 1 & e \\ 0 & 1 \end{smallmatrix}\right)$, $\left(\begin{smallmatrix} 1 & d \\ 0 & 1 \end{smallmatrix}\right)$ (or the other way round) and then down to $\left(\begin{smallmatrix} 0 & 1 \\ -1 & 0 \end{smallmatrix}\right)$, $\left(\begin{smallmatrix} 0 & 1 \\ -1 & 0 \end{smallmatrix}\right)$, so that inverting the procedure proves the theorem. The only point is to show that these operations, or combinations of them, decrease the entries of both matrixes; the claim then follows. When $d, e \geq 2$, which operation works is a matter of the attitude of the long rectangles; when d or $e = 1$, either operation decreases some entries and increases others, but composing the two, in an order determined by attitude, decreases them all. We treat the attitude in terms of the relative sizes of $r, \ldots, h$.

Consider an initial pair

$$\begin{pmatrix} r & a \\ b & s \end{pmatrix} \quad \text{and} \quad \begin{pmatrix} r & g \\ h & s \end{pmatrix}$$

satisfying the rules of the game.

The case $d \geq 2$ and $e \geq 2$ Suppose provisionally that $b < r$. We apply the reduction operation (3.10) to get

$$\begin{pmatrix} r & a \\ b & s \end{pmatrix} \mapsto \begin{pmatrix} b & s \\ db - r & h \end{pmatrix} \quad \text{and} \quad \begin{pmatrix} r & g \\ h & s \end{pmatrix} \mapsto \begin{pmatrix} b & r \\ eh - s & h \end{pmatrix}.$$

We claim that every entry of the two resulting matrices is strictly smaller than the corresponding entry of the initial pair: this holds in the top left entry of either matrix by the case assumption.

Since $rs - ab = 1$, we get $s < a$. By (3.4), $b < r$ implies that $g > r$, and again it is immediate that $s > h$. It remains to consider the two larger entries in the bottom left of the pair.

To see that $eh - s < h$, it is enough to check $hb - 1 < hr$: indeed multiplying by r and substituting for $er = b + g$ and $rs = gh - 1$ gives

$$ehr - rs = h(b + g) - (gh + 1) = bh - 1 < hr.$$

But the inequality $bh - 1 < rh$ holds by the initial assumption.

Similarly we check $db - r < b$ by observing that the equivalent inequality

$$bh - 1 = b(a + h) - (ab + 1) = bds - rs < bs,$$

holds since we already know that $h < s$.

The inequality $db - r < b$ also implies that the resulting matrices have the same attitude, so that if $b, h \geq 1$, the same operation (3.10) will be applied at the next step, but with e, d exchanged, and the descent continues.

The termination condition is that $r = 0$ or $s = 0$, since the inequalities for r, s are the only rules of the game that the reduction operation can break. In either case $ab = -1$, so that $b < r$ and its friends imply $\left(\begin{smallmatrix} r & a \\ b & s \end{smallmatrix}\right) = \left(\begin{smallmatrix} 0 & 1 \\ -1 & 0 \end{smallmatrix}\right)$ and $\left(\begin{smallmatrix} r & g \\ h & s \end{smallmatrix}\right) = \left(\begin{smallmatrix} 0 & 1 \\ -1 & 0 \end{smallmatrix}\right)$. Multiplying by the inverse matrices gives the factorisation (3.5).

Finally, notice that if instead we have $b > r$, then we must have $g < r$ (otherwise both $a < s$ and $h < s$, implying $d = 1$, contrary to the case assumptions), in which case the operation (3.11) performs the required reduction. This gives the factorisation (3.6).

The case $d > 4$ and $e = 1$ The definitions (3.4) imply that $b < r$ and $g < r$. Suppose provisionally that $b < g$.

In this case we apply the reduction operation (3.10) twice, alternating d and e, to see that it reduces the pair. Thus we compute a new pair

$$\begin{pmatrix} 0 & 1 \\ -1 & 1 \end{pmatrix} \begin{pmatrix} 0 & 1 \\ -1 & d \end{pmatrix} \begin{pmatrix} r & a \\ b & s \end{pmatrix} = \begin{pmatrix} db - r & h \\ (d-1)b - r & h - s \end{pmatrix}$$

and

$$\begin{pmatrix} r & g \\ h & s \end{pmatrix} \begin{pmatrix} 1 & 1 \\ -1 & 0 \end{pmatrix} \begin{pmatrix} d & 1 \\ -1 & 0 \end{pmatrix} = \begin{pmatrix} db - r & b \\ (d-2)h - a & h - s \end{pmatrix}.$$

We start knowing $b, g < r$, and so $a, h > s$, together with the case assumption $b < g$, or equivalently $h < a$. So we have $bh - 1 < gh - 1 = rs$. Substituting for h from (3.4) gives $dbs - rs = dbs - ab - 1 < rs$, so $db - r < r$. Similarly $bh - 1 < gh - 1 = rs$, so substituting for b from (3.4) gives $hr - rs = hr - gh - 1 < rs$, so $h - s < s$.

The two longer inequalities remain: $(d-1)b - r < b$ and $(d-2)h - a < h$. For the first, note that $hb - 1 < 2bs$ since $h - s < s$. Substituting for h gives $(d-1)bs - rs < (d-1)bs - ab - 1 = (ds - a)b - bs - 1 < bs$, and dividing by s concludes.

Substituting for h in $h - s < s$ gives $a > (d-2)s$. Since $rs - ab = 1$, $r/b = 1/(bs) + a/s > 1/(bs) + d - 2 > d - 2$ and we have $r > (d-2)b$. Substituting for r now gives $g > (d-2)b$. Since $g/b = a/h$, we get $(d-2)h - a < h$ as required for the second longer inequality.

The same calculations show that $db - r \geq 0$, so that the analogue of the provisional supposition $b < g$ holds again after the two reduction steps, and the descent continues unless we have reached a terminal stage where the inequalities don't hold any more. (Since we jumped straight in with two reduction steps, we should also check whether the inequalities already fail after just one of the steps: by the same calculation, this would only happen if $b = h = 0$, in which case the theorem follows despite the fact that not all matrix entries reduce.)

Finally, if $b > g$ then operation (3.11) applied twice makes the reduction following a similar analysis (in this case a terminal state cannot arise after just one of the steps).

The case $d = 1$, $e > 4$ The definitions (3.4) imply that $a < s$ and $h < s$. Suppose provisionally that $h < a$.

In this case we apply the reduction operation (3.10) twice, alternating d and e, to see that it reduces the pair. Thus we compute a new pair

$$\begin{pmatrix} 0 & 1 \\ -1 & e \end{pmatrix} \begin{pmatrix} 0 & 1 \\ -1 & 1 \end{pmatrix} \begin{pmatrix} r & a \\ b & s \end{pmatrix} = \begin{pmatrix} db - r & h \\ (d-1)b - r & h - s \end{pmatrix}$$

and

$$\begin{pmatrix} r & g \\ h & s \end{pmatrix} \begin{pmatrix} e & 1 \\ -1 & 0 \end{pmatrix} \begin{pmatrix} 1 & 1 \\ -1 & 0 \end{pmatrix} = \begin{pmatrix} db - r & b \\ (d-2)h - a & h - s \end{pmatrix}.$$

The analysis is now virtually identical to the other cases, and we omit it.

4 Combining monomial cones σ_{AB} and σ_{LM}

Here we spell out how the factorisations in the Classification Theorem 3.3 imply growth conditions and congruences on the generators of the varieties V_{AB} and V_{LM}; these are the conditions (i)–(v) of Corollaries 4.2 and 4.7. **From Corollary 4.2(ii) onwards we restrict to the case** $d, e \geq 2$. In Section 5 we also impose $de > 4$, so that we are in the main case of the introduction 1.1. The other cases are treated in [BR2, BR3].

4.1 The Pretty Polytope $\Pi(d, e, k)$

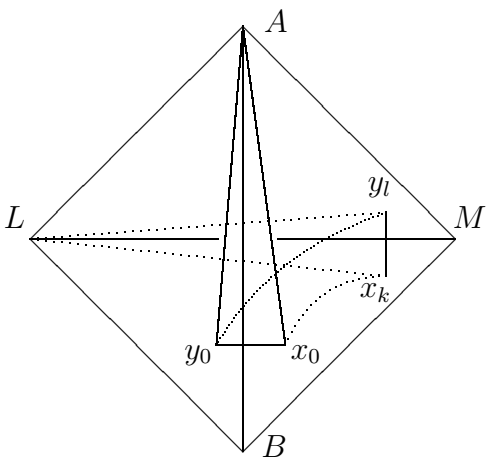

Figure 4.1: Pretty Polytope Π: Starting from simplex $ABLM$, pull out x_0 on plane ABL, etc., with crosspiece x_0y_0 on the edge AB in ratio $1 : d$, and x_ky_l on the edge LM in ratio $1 : e$. Π has 8 vertices and 12 triangular faces; A, B, L, M have valency 5, and x_0, y_0, x_k, y_l valency 4.

All our varieties $T, V_{AB}, V_{LM}, V_{ABLM}$ are equivariant under the same torus $\mathbb{T} = \mathbb{G}_m^4$; write $\mathbb{M} = \mathrm{Hom}(\mathbb{T}, \mathbb{G}_m)$ for its character lattice, identified with the monomial lattice of both V_{AB} and V_{LM}. The coordinate ring of V_{ABLM} constructed in Section 5 is $\mathbb{M}$-graded (that is, $\mathbb{T}$-equivariant). Write $f \overset{\mathbb{T}}{\sim} g$ to mean that f and g are eigenfunctions with the same $\mathbb{T}$-weight or eigenvalue in $\mathbb{M}$. This chapter mostly treats the $\mathbb{T}$-weights of monomials; we mix additive and multiplicative notation, and sometimes write $=$ for $f \overset{\mathbb{T}}{\sim} g$, so that, for example, the first equation of (4.1) means $x_0 \overset{\mathbb{T}}{\sim} L^{-1/d} A^\gamma B^\delta$.

The *Pretty Polytope* Π of Figure 4.1 combines the two polytopes σ_{AB} of 2.3 and σ_{LM} of 3.1. While V_{AB} and V_{LM} each provided many possible $\mathbb{Z}$-bases of $\mathbb{M}$, we use instead

the *impartial* $\mathbb{Q}$-basis L, M, A, B, writing out the $\mathbb{T}$-weights of $x_{0\ldots k}, y_{0\ldots l}$ as follows:

$$x_0 = (-\tfrac{1}{d}, 0, \gamma, \delta) \quad \text{and} \quad x_1 = (0, \tfrac{1}{e}, \alpha, \beta), \tag{4.1}$$

where

$$\begin{pmatrix} \alpha & \beta \\ \gamma & \delta \end{pmatrix} = \begin{cases} \begin{pmatrix} 0 & 1 \\ -1 & e \end{pmatrix} \cdots \begin{pmatrix} 0 & 1 \\ -1 & e \end{pmatrix} \begin{pmatrix} -\frac{1}{d} & 0 \\ 0 & \frac{1}{e} \end{pmatrix} & \text{if } k \text{ is even} \\ \begin{pmatrix} 0 & 1 \\ -1 & e \end{pmatrix} \cdots \begin{pmatrix} 0 & 1 \\ -1 & d \end{pmatrix} \begin{pmatrix} -\frac{1}{e} & 0 \\ 0 & \frac{1}{d} \end{pmatrix} & \text{if } k \text{ is odd} \end{cases} \tag{4.2}$$

(k factors in each product). Compared to (3.6), we simply remove the first and last tags (d at x_k and 0 at x_0), and put in denominators d, e corresponding to the index of the sublattice $\mathbb{M}' = \mathbb{Z} \cdot (L, M, A, B) \subset \mathbb{M}$ (see Corollary 4.7).

The impartial basis gives $\mathbb{M}$ two projections

$$\pi_{AB} \colon \mathbb{M} \to \mathbb{Q}^2 \quad \text{and} \quad \pi_{LM} \colon \mathbb{M} \to \mathbb{Q}^2 \tag{4.3}$$

that track the exponents of A, B and of L, M. The image group $\mathbb{Q}^2$ is partially ordered, and we write $\pi_{LM}(m) \leq 0$ to mean that $m \in \mathbb{M}$ has nonpositive L, M exponents, etc.

Proposition 4.1 *In the impartial basis L, M, A, B, the monomials $x_0, \ldots, y_l$ have $\mathbb{T}$-weights of the form (for even k):*

$$\begin{array}{rcl} x_0 &=& (\ -\frac{1}{d} \quad 0 \quad \gamma \quad \delta\ ) \\ x_1 &=& (\ 0 \quad \frac{1}{e} \quad \alpha \quad \beta\ ) \\ x_2 &=& (\ \frac{1}{d} \quad 1 \quad \cdot \quad \cdot\ ) \\ x_3 &=& (\ 1 \quad d - \frac{1}{e} \quad \cdot \quad \cdot\ ) \end{array} \qquad \begin{array}{rcl} & \cdots & \\ x_{k-2} &=& (\ \cdot \quad \cdot \quad \frac{1}{d} \quad 1\ ) \\ x_{k-1} &=& (\ \alpha \quad \beta \quad 0 \quad \frac{1}{e}\ ) \\ x_k &=& (\ \gamma \quad \delta \quad -\frac{1}{d} \quad 0\ ) \end{array} \tag{4.4}$$

and

$$\begin{array}{rcl} y_0 &=& (\ 0 \quad -\frac{1}{e} \quad d\gamma - \alpha \quad d\delta - \beta\ ) \\ y_1 &=& (\ \frac{1}{d} \quad 1 - \frac{1}{e} \quad \cdot \quad \cdot\ ) \\ & \cdots & \\ y_{j+1} &=& b_j y_j - y_{j-1} \\ & \cdots & \\ y_{l-1} &=& (\ \cdot \quad \cdot \quad \frac{1}{d} \quad 1 - \frac{1}{e}\ ) \\ y_l &=& (\ d\gamma - \alpha \quad d\delta - \beta \quad 0 \quad -\frac{1}{e}\ ) \end{array} \tag{4.5}$$

where the b_j in (4.5) are the tags at y_j (usually 2 or 3).

When k is odd, the top-to-bottom symmetry swaps d and e. At the top, nothing changes (recall that we define $\alpha, \beta, \gamma, \delta$ in x_1, x_0 by the other choice in (4.2)); at the bottom we do $d \leftrightarrow e$ and modify $\alpha, \beta, \gamma, \delta$ accordingly, giving $x_k = (\gamma', \delta', -\frac{1}{e}, 0)$ and $y_l = (e\gamma' - \alpha', e\delta' - \beta', 0, -\frac{1}{d})$.

Proof The matrix product in (4.2) ensures that the $k-1$ changes of basis of the form $x_2 = x_1^e x_0^{-1}$, etc., take the last two entries $\left(\begin{smallmatrix}\alpha & \beta\\ \gamma & \delta\end{smallmatrix}\right)$ of x_1, x_0 into the last two entries $\left(\begin{smallmatrix}-1/d & 0\\ 0 & 1/e\end{smallmatrix}\right)$ of x_k, x_{k-1}. The first two columns then just record known data from V_{LM}, and the last two from V_{AB}. Q.E.D.

Corollary 4.2 *(i) Except for the explicit $-\frac{1}{d}$ and $-\frac{1}{e}$ in x_0, x_k, y_0, y_l at the four corners, all the entries are ≥ 0.*

(ii) (From here on, we assume $d, e \geq 2$.) The L and M exponents $\pi_{LM}(x_i)$ and $\pi_{LM}(y_j)$ increase monotonically with i and j (in fact, increase exponentially *if $de > 4$, as illustrated in Figure 4.2), while $\pi_{AB}(x_i)$ and $\pi_{AB}(y_j)$ decrease.*

(iii) No $x_{0\ldots k}$ or $y_{0\ldots l}$ is $\mathbb{T}$-equivalent to a monomial in the other variables (all the x_i, y_j, A, B, L, M).

For (iii), notice that the x_i, y_j, A and B are minimal generators of the coordinate ring of V_{AB} by the results of 2.3. So it is impossible to write even the first two entries of x_i or y_j as a positive integral combination of the other variables.

Example 4.3 (Case $k = 2$) Then

$$\begin{pmatrix}\alpha & \beta\\ \gamma & \delta\end{pmatrix} = \begin{pmatrix}0 & 1\\ -1 & e\end{pmatrix}\begin{pmatrix}-\frac{1}{d} & 0\\ 0 & \frac{1}{e}\end{pmatrix} = \begin{pmatrix}0 & \frac{1}{e}\\ \frac{1}{d} & 1\end{pmatrix}$$

The variables $x_{0\ldots 2}, y_{0\ldots d}$ are

$$\begin{aligned} x_0 &= (-\tfrac{1}{d}, 0, \tfrac{1}{d}, 1) \\ x_1 &= (0, \tfrac{1}{e}, 0, \tfrac{1}{e}) \\ x_2 &= (\tfrac{1}{d}, 1, -\tfrac{1}{d}, 0) \end{aligned} \qquad \begin{aligned} y_0 &= (0, -\tfrac{1}{e}, 1, d - \tfrac{1}{e}) \\ y_i &= (\tfrac{i}{d}, i - \tfrac{1}{e}, 1 - \tfrac{i}{d}, d - i - \tfrac{1}{e}) \\ &\quad \text{for } i = 0, \ldots, d \\ y_d &= (1, d - \tfrac{1}{e}, 0, -\tfrac{1}{e}) \end{aligned}$$

Check top-to-bottom symmetry. Check the two tag equations at x_0:

$$dx_0 + (1,0,0,0) = x_1 + y_0; \text{ and } 0x_0 + (0,0,1,d) = (0,0,1,d)$$

corresponding to the corner tag equations $x_1 y_0 = x_0^d L$ in V_{LM} and $x_1 y_0 = AB^d$ in V_{AB}. Check the tag equations at y_0: $1y_0 + (0,1,0,0) = x_0 + y_1$, and

$$(e-1)x_1 + (0,0,1,d-1) = (0, 1 - \tfrac{1}{e}, 1, d - \tfrac{1}{e})$$

corresponding to $x_0 y_1 = y_0 M$ in V_{LM} and $x_0 y_1 = x_1^{e-1} AB^{d-1}$ in V_{AB}.

Example 4.4 (Case $k = 3$) Then

$$\begin{pmatrix}\alpha & \beta\\ \gamma & \delta\end{pmatrix} = \begin{pmatrix}0 & 1\\ -1 & e\end{pmatrix}\begin{pmatrix}0 & 1\\ -1 & d\end{pmatrix}\begin{pmatrix}-\frac{1}{e} & 0\\ 0 & \frac{1}{d}\end{pmatrix} = \begin{pmatrix}\frac{1}{e} & 1\\ 1 & e - \frac{1}{d}\end{pmatrix}$$

So $x_{0\ldots3}, y_{0\ldots d+e-2}$ are

$$
\begin{aligned}
x_0 &= (-\tfrac{1}{d}, 0, 1, e-\tfrac{1}{d}) \\
x_1 &= (0, \tfrac{1}{e}, \tfrac{1}{e}, 1) \\
x_2 &= (\tfrac{1}{d}, 1, 0, \tfrac{1}{d}) \\
x_3 &= (1, d-\tfrac{1}{e}, -\tfrac{1}{e}, 0)
\end{aligned}
\qquad
\begin{aligned}
y_0 &= (0, -\tfrac{1}{e}, d-\tfrac{1}{e}, de-2) \\
y_1 &= (\tfrac{1}{d}, 1-\tfrac{1}{e}, d-1-\tfrac{1}{e}, (d-1)e-2+\tfrac{1}{d}) \\
&\ldots \\
y_i &= (\tfrac{i}{d}, i-\tfrac{1}{e}, d-i-\tfrac{1}{e}, (d-i)e-2+\tfrac{i}{d}) \\
&\quad \text{for } i = 0, \ldots, d-1 \\
y_{d-2} &= (1-\tfrac{2}{d}, d-2-\tfrac{1}{e}, 2-\tfrac{1}{e}, 2e-1-\tfrac{2}{d})
\end{aligned}
$$

$$
\begin{aligned}
y_{d-1} &= (1-\tfrac{1}{d}, d-1-\tfrac{1}{e}, 1-\tfrac{1}{e}, e-1-\tfrac{1}{d}) \\
y_d &= (2-\tfrac{1}{d}, 2d-1-\tfrac{2}{e}, 1-\tfrac{2}{e}, e-2-\tfrac{1}{d}) \\
&\ldots \\
y_{d-2+i} &= (i-\tfrac{1}{d}, id-1-\tfrac{i}{e}, 1-\tfrac{i}{e}, e-i-\tfrac{1}{d}) \\
&\quad \text{for } i = 1, \ldots, e \\
y_{d+e-3} &= (e-1-\tfrac{1}{d}, d(e-1)-2+\tfrac{1}{e}, \tfrac{1}{e}, 1-\tfrac{1}{d}) \\
y_{d+e-2} &= (e-\tfrac{1}{d}, de-2, 0, -\tfrac{1}{d})
\end{aligned}
$$

Same checks; note especially the effect of the tag 3 at y_{d-1}.

Example 4.5 (Case $d = 4$, $e = 6$, $k = 6$)

$$
\begin{array}{cccccccc}
 & & & & L & M & A & B & \\
 & x_0 & = & (& -1/4 & 0 & 505/4 & 483 &) \\
6 & x_1 & = & (& 0 & 1/6 & 22 & 505/6 &) \\
4 & x_2 & = & (& 1/4 & 1 & 23/4 & 22 &) \\
6 & x_3 & = & (& 1 & 23/6 & 1 & 23/6 &) \\
4 & x_4 & = & (& 23/4 & 22 & 1/4 & 1 &) \\
6 & x_5 & = & (& 22 & 505/6 & 0 & 1/6 &) \\
 & x_6 & = & (& 505/4 & 483 & -1/4 & 0 &)
\end{array}
\tag{4.6}
$$

and

$$
\begin{array}{cccccccc}
 & & & & L & M & A & B \\
 & y_0 & = & (& 0 & -1/6 & 483 & 11087/6 \;) \\
2 & y_1 & = & (& 1/4 & 5/6 & 1427/4 & 8189/6 \;) \\
2 & y_2 & = & (& 1/2 & 11/6 & 461/2 & 5291/6 \;) \\
3 & y_3 & = & (& 3/4 & 17/6 & 417/4 & 2393/6 \;) \\
2 & y_4 & = & (& 7/4 & 20/3 & 329/4 & 944/3 \;) \\
2 & y_5 & = & (& 11/4 & 21/2 & 241/4 & 461/2 \;) \\
2 & y_6 & = & (& 15/4 & 43/3 & 153/4 & 439/3 \;) \\
3 & y_7 & = & (& 19/4 & 109/6 & 65/4 & 373/6 \;) \\
2 & y_8 & = & (& 21/2 & 241/6 & 21/2 & 241/6 \;) \\
3 & y_9 & = & (& 65/4 & 373/6 & 19/4 & 109/6 \;) \\
2 & y_{10} & = & (& 153/4 & 439/3 & 15/4 & 43/3 \;) \\
2 & y_{11} & = & (& 241/4 & 461/2 & 11/4 & 21/2 \;) \\
2 & y_{12} & = & (& 329/4 & 944/3 & 7/4 & 20/3 \;) \\
3 & y_{13} & = & (& 417/4 & 2393/6 & 3/4 & 17/6 \;) \\
2 & y_{14} & = & (& 461/2 & 5291/6 & 1/2 & 11/6 \;) \\
2 & y_{15} & = & (& 1427/4 & 8189/6 & 1/4 & 5/6 \;) \\
 & y_{16} & = & (& 483 & 11087/6 & 0 & -1/6 \;)
\end{array}
\tag{4.7}
$$

We read this table in several ways. Omitting the A and B columns describes σ_{LM} in the impartial basis. Notice the tag equations

bottom: $x_1 y_0 = x_0^4 L$ and $x_0 y_1 = y_0 M$;
sides: $x_0 x_2 = x_1^6$, $x_1 x_3 = x_2^4$ and so on;
top: $x_5 y_{16} = L^{505} M^{1932}$ and $x_6 y_{15} = x_5^5 L^{373} M^{1427}$.

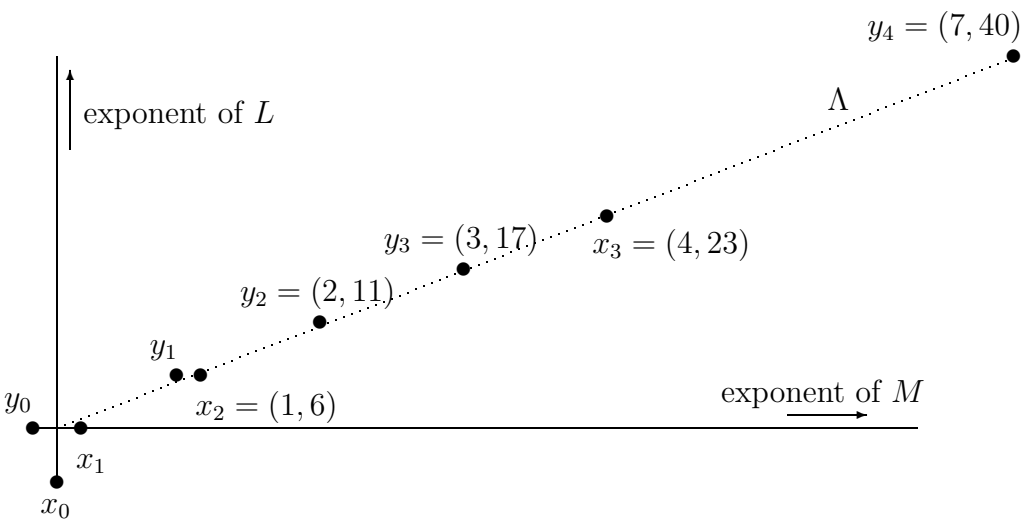

Figure 4.2: Scissors (compare the dots of Figure 2.2.b). The exponents of L are in units of $1/4$ and those of M in units of $1/6$. The initial points are $x_0 = (-1, 0)$, $y_0 = (0, -1)$, $x_1 = (0, 1)$, $y_1 = (1, 5)$.

Figure 4.2 plots the first two columns of (4.7) as "scissors" controlled by the points $x_0 = (-\frac{1}{d}, 0)$ and $y_0 = (0, -\frac{1}{e})$ and the origin $(0,0)$ (implicit but crucial). To describe it in words, the sequence of y_i starts from y_0 and tries to grow along the line Λ of slope $1/[4,6,4,6,\dots] \doteq 0.261387212$, without crossing it. It first tries x_0 (slope $-\infty$), then x_1 (slope 0) and x_2 (slope 1/4, so under Λ), then takes one step back to $y_1 = x_2 y_0$ (slope 3/10, so above Λ). Now y_0, y_1, y_2, y_3, x_3 is an arithmetic progression of length $5 = d+1$ with increment x_2 (and $y_{i+1} = y_i x_2$, so $0y_0y_1x_2$, $0y_1y_2x_2$, etc., are parallelograms); but x_3 (slope 6/23) is below L; so take one step back to y_3 and construct the next arithmetic progression $y_3, y_4, y_5, y_6, y_7, x_4$ of length $6 = e$ with increment x_3, and so on. Compare Figure 2.2, where the scissors were more open.

Remark 4.6 The abstract continued fraction $[e, d, \dots]$ and its complementary continued fraction $[2, 2, \dots, 3, \dots]$ has two different "scissors" embeddings into the L, M-plane (as the dots of Figures 2.2 and 4.2) and into the A, B-planes, and the Pretty Polytope $\Pi(d, e, k)$ is just the diagonal embedding into the product.

4.2 The quotient Q and the Padded Cell

The exponents of $x_{0\dots k}, y_{0\dots l}$ in Proposition 4.1 also behave in a characteristic way modulo the integers (see Figure 4.3). To understand this, we write $\mathbb{M}' = \mathbb{Z} \cdot (L, M, A, B) \subset \mathbb{M}$ for the sublattice generated by A, B, L, M, and $Q = \mathbb{M}/\mathbb{M}'$ for the quotient. We think of Q pictorially as a fundamental domain in $\mathbb{M}$ for the translation lattice $\mathbb{M}'$, as in Figure 4.3.

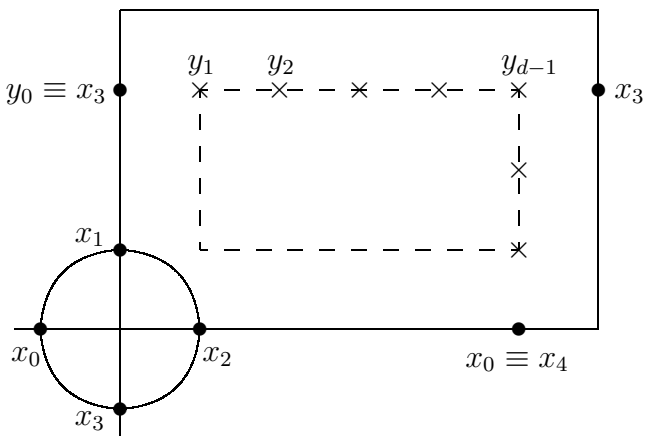

Figure 4.3: The Padded Cell (with sides identified): the values of x_i and y_j in the torus $Q = \mathbb{M}/\mathbb{M}'$. The x_i cycle around the 4 points $(\pm\frac{1}{d}, 0)$ and $(0, \pm\frac{1}{e})$ closest to the origin, while the y_i walk around the path of Figure 4.3, performing $k-1$ quarter-circuits around the padding of the cell, starting from $x_3 \equiv y_0$. Each quarter-circuit takes place in steps of x_i and has endpoint x_{i+1}.

Corollary 4.7 *(iv)* $\mathbb{Q} \cong \mathbb{Z}/d \oplus \mathbb{Z}/e$, *based by:*

if $k = 2\kappa$ is even:

$$x_0 \equiv (-\tfrac{1}{d}, 0, \mp\tfrac{1}{d}, 0); \quad \textit{and} \quad y_0 \equiv (0, -\tfrac{1}{e}, 0, \pm\tfrac{1}{e}); \tag{4.8}$$

if $k = 2\kappa + 1$ is odd:

$$x_0 \equiv (-\tfrac{1}{d}, 0, 0, \pm\tfrac{1}{d}) \quad \textit{and} \quad y_0 \equiv (0, -\tfrac{1}{e}, \pm\tfrac{1}{e}, 0), \tag{4.9}$$

where in either case $\pm = (-1)^\kappa$.

(v) The classes in Q of monomials $x_0, \dots, y_l$ are given as follows (for even k):

$$\begin{gathered} x_1 \equiv -y_0 \equiv (0, \tfrac{1}{e}, 0, \mp\tfrac{1}{e}), \quad x_i \equiv -x_{i-2} \quad \textit{for } i \geq 2 \\ \textit{and} \quad y_{j+1} = y_j + x_{i(j)} \end{gathered} \tag{4.10}$$

for j in the appropriate interval. In particular, in Q, the x_i are periodic with period 4, with $x_3 \equiv y_0$.

Note that in Q, the different corner tags on the two long rectangles say the same thing; thus

$$\begin{gathered} x_1 y_0 = x_1^0 A^\alpha B^\beta = x_0^d L \quad \text{both give} \quad x_1 \equiv y_0^{-1} \in Q \\ x_0 y_1 = y_0^{-(e-1)} A^\gamma B^\delta = y_0 M \quad \text{both give} \quad y_0 \equiv x_0 y_1 \in Q \end{gathered}$$

because $x_0^d, y_0^e \in \mathbb{M}$.

5 Proof of Theorem 1.1: main case

We prove the existence of the diptych variety V_{ABLM} for any pair of toric extensions of the tent $V_{AB} \supset T \subset V_{LM}$ arising from the Classification Theorem 3.3 **under the assumption that** $d, e \geq 2$ **and** $de > 4$.

5.1 Structure of the proof

The proof of Theorem 1.1 builds a staircase: first, we drop a chain of projections down from the top of V_{AB} to eliminate the generator $x_{2\dots k}$ and $y_{2\dots l}$ one at a time. This chain will serve as a guiding rail in the main construction; it records the order of variables and the current state of the tags and annotations as we eliminate them (Proposition 5.2): as each $s_\nu = x_{i+1}$ or y_{j+1} is eliminated from $V_{AB,\nu+1}$, it has tag 1, and appears in an equation $s_\nu h_\nu = x_i y_j$ with its neighbours, where $h_\nu = h_\nu(A, B)$ is the monomial in A, B defined in 5.2.3.

We then build the 6-fold V_{ABLM} up from the bottom, holding tight to our guiding rail, the chain of projections of V_{AB}. Each step $V_{\nu+1} \to V_\nu$ of the induction is a Kustin–Miller unprojection (see [PR]), and adjoins an unprojection variable $s_\nu = x_{i+1}$ or y_{j+1}. The

current V_ν is contained in the ambient space $\mathbb{A}_\nu = \mathbb{A}^{i+j+6}_{\langle x_{0\dots i}, y_{0\dots j}, A, B, L, M\rangle}$. The main point is to set up the unprojection divisor $D_\nu \subset V_\nu$; we *define* it by the ideal

$$I_{D_\nu} = (x_{0\dots i-1}, y_{0\dots j-1}, h_\nu), \tag{5.1}$$

with $h_\nu(A, B)$ as in 5.2.3, so that D_ν is the hypersurface

$$D_\nu : (h_\nu(A, B) = 0) \subset \mathbb{A}^6_{\langle x_i, y_j, A, B, L, M\rangle}. \tag{5.2}$$

Thus D_ν is by definition the product of affine 4-space $\mathbb{A}^4_{\langle x_i, y_j, L, M\rangle}$ with the monomial curve $h_\nu(A, B) = 0$; the elements L, M form a regular sequence for D_ν, and the section $L = M = 0$ in D_ν is the unprojection divisor $D_{AB,\nu}$ for $V_{AB,\nu+1} \to V_{AB,\nu}$. The remaining issue is to prove that $D_\nu \subset V_\nu$, or equivalently, that

$$I_{V_\nu} \subset I_{D_\nu} = \big(x_{0\dots i-1}, y_{0\dots j-1}, h_\nu\big). \tag{5.3}$$

For this, rather than working with the actual equations of V_ν (that we cannot always calculate in closed form, and include complicated terms), we prove the stronger result: *any monomial in $x_{0\dots i}, y_{0\dots j}, A, B, L, M$ with the same $\mathbb{T}$-weight as a generator of I_{V_ν} is in $I_{D_\nu} = (x_{0\dots i-1}, y_{0\dots j-1}, h_\nu)$.* Thus, every $\mathbb{T}$-homogeneous generator of I_{V_ν} is a sum of monomials in I_{D_ν}.

It turns out in the end, much to our regret, that our proof does here not involve any explicit pentagrams or Pfaffians; however, they are important in the constructions of [BR2] when $de = 4$.

5.2 The projection sequence of V_{AB}

This section and the next set out facts and notation for the chains of birational projections down from V_{AB} and up from V_{LM}. Either chain is provided by the blowdown of Proposition 2.1(d) applied to the conclusion $[a_2, \dots, b_1] = 0$ of Corollary 2.8.

Example 5.1 Consider the long rectangle of Figure 1.2. The concatenated continued fraction $[4, 2, 1, 3, 2, 2] = 0$ is deconstructed as

$$[4, \underline{2, 1, 3}, 2, 2] \mapsto [\underline{4, 1, 2}, 2, 2] \mapsto [\underline{3, 1, 2}, 2] \mapsto [\underline{2, 1, 2}] \mapsto [1, 1] = 0$$

This is a recipe for a chain of birational projections, each eliminating a monomial from σ_{AB} with tag 1:

$$\begin{array}{ll} & 1\,B \\ A & 2 \\ & 3 \\ & 4 \\ & 2 \\ & 2 \\ & 0 \\ & -1 \end{array} \mapsto \begin{array}{lll} & & \\ AB & 1 & 2\,B \\ & 4 & 2 \\ & 2 & 2 \\ & 0 & -1 \end{array} \mapsto \begin{array}{lll} & & \\ AB & 3 & 1\,AB^2 \\ & 2 & 2 \\ & 2 & 2 \\ & 0 & -1 \end{array} \mapsto$$

$$\begin{array}{lll} & & \\ A^2B^3 & 2 & 1\,AB^2 \\ & 2 & 2 \\ & 0 & -1 \end{array} \mapsto \begin{array}{lll} & & \\ A^3B^5 & 1 & \\ & 2 & 1\,AB^2 \\ & 0 & -1 \end{array} \mapsto \begin{array}{lll} & & \\ A^3B^5 & 1 & 0\,A^4B^7 \\ & 0 & -1 \end{array}$$

For example, on the second line, we read $x_1y_2 = x_2^2A^2B^3$ and $x_2y_1 = y_2AB^2$ from the tags and annotation of the first rectangle, that we can check against (1.7). Each rectangle is the monomial cone $\sigma_{AB,\nu}$ of a Gorenstein affine toric variety $V_{AB,\nu}$ with the given monomials in A, B as annotations, and each step $V_{AB,\nu+1} \to V_{AB,\nu}$ is a birational projection.

5.2.1 Order of monomials

Our construction inverts this type of chain, up from a codimension 2 complete intersection in x_0, x_1, y_0, y_1, A, B, adding x_2, y_2 and so on one at a time, to recover V_{AB}. For this, we order the $k + l - 2$ steps *inverse to the elimination* of the monomials $x_{2\ldots k}, y_{2\ldots l}$; that is, we rename the nth eliminated monomial s_ν with $\nu = k + l - 2 - n$, so that $s_0 = x_2$ and $s_1 = y_2$. We work by induction on this ν. At the same time, we name the annotation h_ν on the monomial s_ν as it is eliminated; the chain starts from the top with

$$s_{k+l-3} = y_l \quad \text{and} \quad h_{k+l-3} = B \quad \text{and} \quad b_l = 1. \tag{5.4}$$

(This uses the main case hypothesis $d, e \geq 2$ so that $b_l = 1$.)

Thus in Example 5.1, $[s_0, s_1, s_2, s_3, s_4] = [x_2, y_2, y_3, x_3, y_4]$ and

$$[h_0, h_1, h_2, h_3, h_4] = [A^3B^5, AB^2, AB^2, AB, B].$$

The scissors of Figure 4.2 strongly suggest this ordering of the monomials, although there is a choice to make at the end between y_1 and x_2, which both have tag 1; we always eliminate $s_1 = x_2$.

5.2.2 The projection $V_{AB,\nu+1} \to V_{AB,\nu}$ and the bar x_i——y_j

The projection sequence gives cones $\sigma_{AB,\nu}$ that depend on the induction parameter ν. The top corners of each $\sigma_{AB,\nu}$ are monomials x_i and y_j with $i = i(\nu)$ and $j = j(\nu)$ (Table 5.1 keeps track of these functions), and we know the equations of $V_{AB,\nu}$ including

$$x_{i-1}y_j = x_i^{\alpha_\nu}A_\nu \quad \text{and} \quad x_iy_{j-1} = y_j^{\beta_\nu}B_\nu, \tag{5.5}$$

given by the tags and annotations at x_i and y_j in $V_{AB,\nu}$ as in Figure 5.1. We think of this action happening at the top of a sub-rectangle, which we refer to as the *bar* x_i——y_j; the bar cascades down the long rectangle as variables are projected away (see Figure 5.2), and the tag equations (5.5) at each bar provide the key pieces of quantitative data about the convexity of V_{AB} that we use throughout the proof.

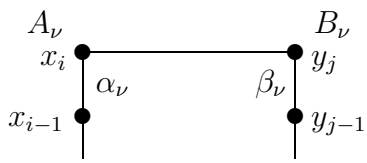

Figure 5.1: The *bar* x_i——y_j at the top of $\sigma_{AB,\nu}$, with tag equations (5.5).

Proposition 5.2 *The chain of projections $V_{AB,\nu+1} \to V_{AB,\nu}$ reduces V_{AB} down to a codimension 2 complete intersection $V_{AB,0} \subset \mathbb{A}^6_{\langle x_0,x_1,y_0,y_1,A,B\rangle}$. The step $V_{AB,\nu+1} \to V_{AB,\nu}$ eliminates $s_\nu = x_{i+1}$ or y_{j+1}, with two possible cases for the top of $\sigma_{AB,\nu+1}$:*

$$\begin{array}{cccccc} & s_\nu & & & & s_\nu \\ \textit{either} & x_i & y_j & \textit{or} & x_i & y_j \\ & x_{i-1} & y_{j-1} & & x_{i-1} & y_{j-1} \end{array}$$

In the left case $s_\nu = x_{i+1}$, the top of $\sigma_{AB,\nu}$ and of $\sigma_{AB,\nu+1}$ are related by

$$A_\nu = A_{\nu+1},\ \ B_\nu = A_{\nu+1}B_{\nu+1},\ \ \alpha_{\nu+1} = 1,\ \ \alpha_\nu = a_i - 1,\ \ \beta_\nu = \beta_{\nu+1} - 1, \tag{5.6}$$

and similarly in the right case by

$$A_\nu = A_{\nu+1}B_{\nu+1},\ \ B_\nu = B_{\nu+1},\ \ \alpha_\nu = \alpha_{\nu+1} - 1,\ \ \beta_{\nu+1} = 1,\ \ \beta_\nu = b_j - 1. \tag{5.7}$$

5.2.3 Choice of $h_\nu(A,B)$ and the unprojection divisor $D_{AB,\nu} \subset V_{AB,\nu}$

Proposition 5.2 described the projection $V_{AB,\nu+1} \to V_{AB,\nu}$ that eliminates the variable s_ν; inverting this, we construct $V_{AB,\nu+1}$ as an unprojection from $V_{AB,\nu}$ adjoining s_ν. For this, we set $h_\nu = \mathrm{hcf}(A_\nu, B_\nu)$, equal to A_ν or B_ν by (5.6–5.7) and define $D_{AB,\nu} \subset \mathbb{A}^{i+j+4}_{\langle x_{0\dots i}, y_{0\dots j}, A, B\rangle}$ by the ideal $(x_{0\dots i-1}, y_{0\dots j-1}, h_\nu)$; thus $D_{AB,\nu}$ is the hypersurface $(h_\nu = 0) \subset \mathbb{A}^4_{\langle x_i, y_j, A, B\rangle}$.

Claim *The ideal of $V_{AB,\nu}$ is contained in the ideal $(x_{0\dots i-1}, y_{0\dots j-1}, h_\nu)$ of $D_{AB,\nu}$, or in other words, $D_{AB,\nu} \subset V_{AB,\nu}$.*

Proof We know that $I_{V_{AB,\nu}}$ is generated by equations for $x_{i'}y_{j'}$, $x_{i'}x_{i''}$ and $y_{j'}y_{j''}$ for suitable values of the indexes i', i'', j', j''. Consider for example an equation $x_i y_{j'} = x_i^\xi y_j^\eta A^\alpha B^\beta$ for some $j' < j$. First $\xi = 0$, for otherwise dividing by x_i gives a monomial expression for $y_{j'}$ that contradicts Figure 2.3, where $\langle y_{0\dots l}\rangle$ is a 2-face of σ_{AB}. Substitute for x_i from the tag equation $x_i y_{j-1} = y_j^{\beta_j} B_\nu$ to give

$$y_{j'} y_j^{\beta_j - \eta} y_{j-1}^{-1} = A^\alpha B^\beta B_\nu^{-1}. \tag{5.8}$$

Now both sides of (5.8) are 1, since the 4-dimensional vector space $\mathbb{M}_\mathbb{Q}$ is the direct sum of the 2-dimensional subspace spanned by $y_{0\dots l}$ and that spanned by A, B (compare Figure 2.3). Therefore $A^\alpha B^\beta = B_\nu$, and both sides of our equation are in the ideal. The other equations are similar. Q.E.D.

The initial case $n = 0$ or $\nu = k + l - 2$ is $V_{AB,\nu} = V_{AB}$; in our construction of V_{ABLM}, it is the final goal: if we reach it, there is nothing more to check. Then $A = A_\nu$, $B = B_\nu$, $h_\nu = 1$, and divisibility by h_ν is trivial.

5.3 Crosses, pitchforks and pentagrams

5.3.1 The spreadsheet for V_{AB}

Our construction of $V_{\nu+1}$ from V_ν reverses the projection sequence down from the top of V_{AB}. Our proof also needs information derived from the projection sequence up from the bottom of V_{LM}. Thus in Extended Example 1.2, we deconstructed V_{LM} by eliminating y_0, y_1, y_2, x_0, x_1 from the bottom of Figure 1.3. Here we establish how the two projection sequences interleave, as an exercise in patient bookkeeping.

Table 5.1 gives the function $i = i(\nu)$, $j = j(\nu)$ of 5.2.2 describing the top of $V_{AB,\nu}$ as in Figure 5.1. The table repeats periodically with period $d+e-2$, or alternate half periods of $d-1$, $e-1$. We set $v = \nu \bmod d+e-2$ and write $\nu = C(d+e-2)+v$.

v	i	j	
0	$2C+1$	$(d+e-4)C+1$	
a	$2C+2$	$(d+e-4)C+a$	for $1 \le a \le e-1$
$e+b-1$	$2C+3$	$(d+e-4)C+e-2+b$	for $1 \le b \le d-1$
Final	$k = 2\kappa+1$	$l = (d+e-4)\kappa+2$	

v	i	j	
0	$2C+1$	$(d+e-4)C+1$	
a	$2C+2$	$(d+e-4)C+a$	for $1 \le a \le d-1$
$d+b-1$	$2C+3$	$(d+e-4)C+d-2+b$	for $1 \le b \le e-1$
a	$2C+2$	$(d+e-4)C+a$	for $1 \le a \le d-1$
Final	$k = 2\kappa$	l	

Table 5.1: Numbering the unprojection sequence for V_{AB}. The even case $k = 2\kappa$ has one fewer half round. The final line is irregular: it adds a final y_l instead of x_{k+1} with $l = (d+e-4)\kappa+2$ or $l = (d-2)\kappa+(e-2)(\kappa-1)+2$.

The starting point $\nu = 0$ is $V_{AB,\nu}$ with x_1, y_1 at its top bar. The table is split into two, the k odd and k even cases; we describe the odd case $k = 2\kappa+1$. Set $C = 0$ and enter the first round: the line $v = a = 1$ adds an x_i, then $a = 2, \dots, e-1$ is a half round that adds $e-2$ terms y_j; similarly, the line $v = e$ (so $b = 1$) adds an x_i and then $b = 2, \dots, d-1$ is a half round that adds $d-2$ terms y_j. We then increment $C \mapsto C+1$ and loop. Each half round adds one x_i and $d-2$ or $e-2$ terms y_j. There are $k-1$ half rounds, ending with $\nu = (d+e-2)\kappa$ if $k = 2\kappa+1$ or $\nu = (d-1)\kappa+(e-1)(\kappa-1)$ if $k = 2\kappa$.

The above treatment assumes that we are in the main case $d, e \ge 2$; everything remains true when d or e or both are 2. Then the intervals $2 \le a \le d-1$ or $2 \le b \le e-1$ are

empty, so the corresponding half periods add one x_i and no y_j.

5.3.2 Comparing the projection sequences for V_{AB} and V_{LM}

We want to compare the bars x_i, y_j at the top of $V_{AB,\nu}$ with the corresponding thing at the bottom of V_{LM} after a number of projections. To see this, we divide the monomials y_j up into intervals according to the lines of Table 5.1, writing Y_{i-1} for the ith half period.

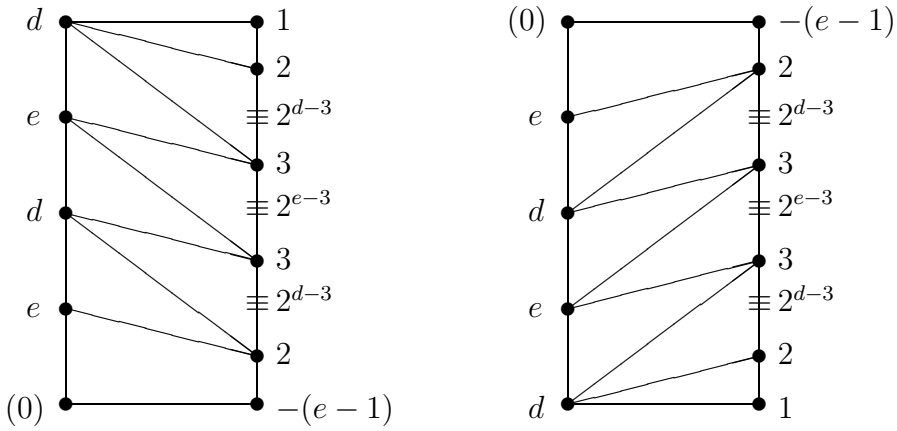

Figure 5.2: Projecting V_{AB} from the top and V_{LM} from the bottom

In more detail, for k even, the line for even $i = 2C + 2$ gives the interval

$$Y_{i-1} = \left\{ y_j \;\middle|\; \text{for } j \in [n_i + 1, \ldots, n_i + d - 1] \right\} \tag{5.9}$$

where $n_i = (d + e - 4)\frac{i-2}{2}$; similarly, the line $i' = 2C + 3$ gives

$$Y_{i'-1} = \left\{ y_j \;\middle|\; \text{for } j \in [n_{i'} + 1, \ldots, n_{i'} + e - 1] \right\} \tag{5.10}$$

where $n_{i'} = (d + e - 4)\frac{i'-3}{2} + d - 2$.

Notice the adjacency between the intervals: the last entry $n_i + d - 1$ of Y_{i-1} equals the first entry $n_{i'} + 1$ of the following interval $Y_{i'}$ with $i' = i + 1$, and vice versa. For d or $e = 2$, the interval Y_i reduces to one element (which, in Figure 5.2, is tagged with 4, rather than 3).

Lemma 5.3 *The bars at the top of $V_{AB,\nu}$ are precisely x_{i+1}, y_j with $j \in Y_i$.*

The bars at the bottom of $V_{LM,\nu'}$ (after projecting out ν' monomials from V_{LM}, starting with y_0) are precisely x_{i-1}, y_j with $j \in Y_i$. See Figure 5.2.

The first clause is a more digestible rephrasing of the information contained in Table 5.1 about the order of projection. The projection sequence of V_{LM} from the bottom is enumerated by a symmetric spreadsheet, which proves the second clause.

The following simple consequence is a key point of our proof in 5.4.

Corollary 5.4 *Suppose that we project out n_1 monomials from the top of V_{AB} down to the top bar x_i, y_j and n_2 monomials from the bottom of V_{LM} up to the bottom bar $x_{i'}, y_{j'}$, where $n_1 + n_2 = k + l - 2$, so that just 4 monomials remain. Then $i' < i$ and $j' \le j$.*

Equivalently, either $i' = i - 1$ and $j' = j - 1$ or $i' = i - 2$ and $j' = j$, so that any such projection leads to a "cross" or "pitchfork" of the shape

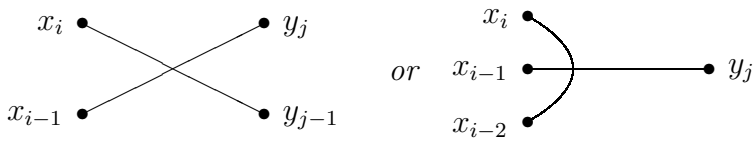

(5.11)

The same phenomenon was already implicit in the cascade of pentagrams of Example 1.2; we include this, although it is not essential for our proof.

Corollary 5.5 *Projecting out n_1 monomials from the top of V_{AB} and n_2 from the bottom of V_{LM} with $n_1 + n_2 = k + l - 3$ gives a pentagram of one of the two shapes*

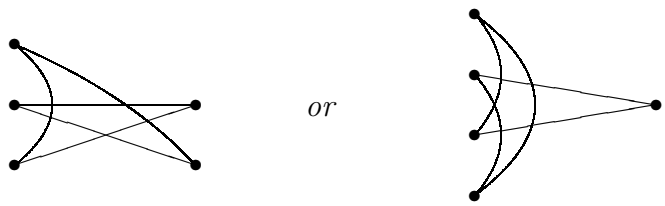

(5.12)

5.4 Proof by induction

We construct $V = V_{ABLM}$ by serial unprojection. The induction starts from the codimension 2 complete intersection

$$V_0 \subset \mathbb{A}^8_{\langle x_0, x_1, y_0, y_1, A, B, L, M\rangle}$$

defined by

$$x_1 y_0 = T_{x_0}(V_{AB}) + T_{x_0}(V_{LM}) \quad \text{and} \quad x_0 y_1 = T_{y_0}(V_{AB}) + T_{y_0}(V_{LM})$$

where $T_{x_0}(V_{AB})$ is the righthand side of the tag equation at x_0 in V_{AB}, and similarly for the other three terms. Clearly V_0 is Gorenstein and A, B, L, M is a regular sequence, with the regular section $L = M = 0$ in V_0 the variety $V_{AB,0}$. We use the following elementary fact about unprojection.

Lemma 5.6 *Unprojection commutes with regular sequences: let X, D be as in [PR], Theorem 1.1 and $Y \to X$ the unprojection of D in X. Suppose that $z_1, \dots, z_r \in \mathcal{O}_X$ is a regular sequence for X and for D. Then $z_1, \dots, z_r$ is also a regular sequence for $\mathcal{O}_Y$, and Y_z is the unprojection of D_z in X_z, where $Y_z : (z_1 = \cdots = z_r = 0) \subset Y$ and similarly for D_z and X_z.* $\square$

Inductive assumption 5.7 *We own a variety $V_\nu = V_{ABLM,\nu}$ having a $\mathbb{T}$-action, together with a regular sequence L, M made up of $\mathbb{T}$-eigenfunctions such that $V_\nu \cap (L = M = 0) = V_{AB,\nu}$.*

We start with $\nu = 0$, and $V_{ABLM,\nu} = V_0$ as above. The induction has $k + l - 2$ steps, adjoining $x_{2\ldots k}$ and $y_{2\ldots l}$ in the order determined in 5.2.1. When ν reaches $k + l - 2$ then $V_{ABLM} = V_\nu$ and we are finished. Otherwise, if $\nu < k + l - 2$, the induction step consists of proving that V_ν has a divisor D_ν on which L, M is a regular sequence, and the section $D_\nu \cap (L = M = 0)$ is the divisor $D_{AB,\nu} \subset V_{AB,\nu}$.

If $\nu < k+l-2$, by 5.2.3, the step $V_{AB,\nu+1} \to V_{AB,\nu}$ of the chain down from V_{AB} is the unprojection adjoining the element s_ν with unprojection ideal $\big(x_{0\ldots i-1}, y_{0\ldots j-1}, h_\nu\big)$, where h_ν is the monomial in A, B defined in 5.2.3. We seek to imitate this for the 6-fold V_ν; for this, define D_ν by

$$D_\nu \subset \mathbb{A}^8_{\langle x_{0\ldots i}, y_{0\ldots j}, A, B, L, M\rangle} \quad \text{with ideal} \quad I_{D_\nu} = \big(x_{0\ldots i-1}, y_{0\ldots j-1}, h_\nu\big).$$

Clearly, it is the hypersurface $D_\nu : (h_\nu = 0) \subset \mathbb{A}^6_{\langle x_i, y_j, A, B, L, M\rangle}$, and is the product of $\mathbb{A}^4_{\langle x_i, y_j, L, M\rangle}$ with the plane curve $h_\nu(A, B) = 0$. The issue is to prove that $D_\nu \subset V_\nu$.

Proposition 5.8 (Key point) *$I_{V_\nu} \subset I_{D_\nu} = (x_{0\ldots i-1}, y_{0\ldots j-1}, h_\nu)$ for every $\nu < k + l - 2$.*

We prove this by a general argument on $\mathbb{T}$-weights of monomials that may appear in a relation, without any need to analyse the actual equations of V_ν. We introduce the notation $R(\nu)$ for the $\mathbb{T}$-weights of homogeneous generators of $I_{V_{AB,\nu}}$ or equivalently, of I_{V_ν} (by $\mathbb{T}$-equivariance); we write $f \in R(\nu)$ to indicate that f is a homogeneous polynomial with $\mathbb{T}$-weight in $R(\nu)$. The precise statement we prove is the following:

Claim 5.9 *Any monomial $x_i^\xi y_j^\eta A^\alpha B^\beta L^\lambda M^\mu \in R(\nu)$ is divisible by h_ν. (We emphasise the prevailing hypotheses: $d, e \geq 2$ and $de > 4$.)*

Recall that $h_\nu = \mathrm{hcf}(A_\nu, B_\nu)$; we usually prove divisibility by A_ν or B_ν. By definition, any alleged monomial in $R(\nu)$ is $\mathbb{T}$-equivalent to a relation in $I_{V_{AB,\nu}}$ for $x_{i'}y_{j'}$ or $x_{i'}x_{i''}$ or $y_{j'}y_{j''}$. The main mechanism of the proof is to compare it with one of the two equations (5.5), or more precisely, with one of the model monomials

$$x_{i-1}y_j \overset{\mathbb{T}}{\sim} x_i^{\alpha_\nu} A_\nu \quad \text{and} \quad x_i y_{j-1} \overset{\mathbb{T}}{\sim} y_j^{\beta_\nu} B_\nu, \tag{5.13}$$

coming from the top corners of $V_{AB,\nu}$ as in Figure 5.1.

Step 1 *Claim 5.9 holds for every monomial in $R(\nu - 1)$.* Indeed, it is divisible by $h_{\nu-1}$ by induction, and by (5.6–5.7) the h_ν increase as ν decreases.

Step 2 The first actual calculation in the proof: *Claim 5.9 holds for all the monomials $x_{i'}y_j$ with $i' = 0, \ldots, i-1$ and $x_i y_{j'}$ with $j' = 0, \ldots, j-1$ appearing in* cross-over *relations.*

Proof We write out the proof for $x_{i'}y_j$ in detail as a model case. The method is to compare an alleged monomial

$$x_i^\xi y_j^\eta m \overset{\mathbb{T}}{\sim} x_{i'}y_j \in R(\nu), \quad \text{where } m \text{ is a monomial in } A, B, L, M$$

with the known monomial $x_i^{\alpha_\nu} A_\nu \overset{\mathbb{T}}{\sim} x_{i-1}y_j$ from (5.13). (Of course, we never need consider monomials which involve x or y variables from I_{D_ν}.) We have $\eta = 0$: otherwise dividing both sides by y_j contradicts Corollary 4.2(iii). Consider

$$\frac{x_{i'}}{x_{i-1}} \overset{\mathbb{T}}{\sim} x_i^{\xi-\alpha_\nu} \frac{m}{A_\nu}. \tag{5.14}$$

By Corollary 4.2(ii) and the fact that $i' \leq i-1$, the lefthand side has L, M exponents $\pi_{LM}(\frac{x_{i'}}{x_{i-1}}) \leq 0$ (see (4.3) for the notation π_{LM} and π_{AB}); thus $\alpha_\nu \geq \xi$, and the equivalence takes the form

$$x_i^{\alpha_\nu-\xi} \frac{x_{i'}}{x_{i-1}} \overset{\mathbb{T}}{\sim} \frac{m}{A_\nu} \quad \text{with} \quad \alpha_\nu \geq \xi. \tag{5.15}$$

Now for the same reason, $\pi_{AB}(\frac{x_{i'}}{x_{i-1}}) \geq 0$. The same goes for $x_i^{\alpha_\nu-\xi}$, except for the case $x_i = x_k$, at the top left of the rectangle for V_{AB}. In the former case, we are done: $\pi_{AB}(m/A_\nu) \geq 0$ so m is divisible by A_ν as required.

The initial case $x_i = x_k$ is important: $\pi_{AB}(x_k) = (-\frac{1}{d}, 0)$ by Proposition 4.1; because of the negative exponent, we cannot get our conclusion by convexity alone. Instead we use a congruence argument on the Padded Cell Figure 4.3: in fact, the negative exponent is the smallest possible value $-\frac{1}{d}$, and we claim that α_ν is one of $d-1, d-2, \ldots, 1$. Indeed, if $\nu = k+l-2$ we are at the end of the induction, and there is nothing to prove. Otherwise, the tag at x_k has decreased by at least one from its pristine value d. It follows that the lefthand side of (5.15) has A exponent > -1 and B exponent ≥ 0. On the other hand, the righthand side of (5.15) is a Laurent monomial. Therefore also in the initial case m is divisible by A_ν, as required.

The argument for $x_i y_{j'}$ is similar but slightly easier. Suppose that

$$x_i y_{j'} \overset{\mathbb{T}}{\sim} x_i^\xi y_j^\eta m \quad \text{with} \quad m = A^\alpha B^\beta L^\lambda M^\mu. \tag{5.16}$$

First $\xi = 0$, because otherwise dividing through by x_i would contradict Corollary 4.2(iii). Next, dividing through by the monomials in the second expression of (5.13) gives

$$\frac{y_{j'}}{y_{j-1}} = y_j^{\eta-\beta_\nu} \times \frac{m}{B_\nu}. \tag{5.17}$$

As before, since $j' \leq j-1$, Corollary 4.2(ii) gives that $\pi_{LM}(\frac{y_{j'}}{y_{j-1}}) \leq 0$. Therefore $\eta - \beta_\nu \leq 0$. Taking that term to the lefthand side gives

$$y_j^{\beta_\nu-\eta} \frac{y_{j'}}{y_{j-1}} = \frac{m}{B_\nu} \quad \text{with} \quad \beta_\nu \geq \eta. \tag{5.18}$$

Now $j' \le j-1$, so $\pi_{AB}(\frac{y_{j'}}{y_{j-1}}) \ge 0$; the same goes for y_j except if $j = l$ and y_j is at the top of the long rectangle, and we are finished, with $V_\nu = V_{ABLM}$. Therefore the exponents of A, B on the lefthand side are ≥ 0, and hence m is divisible by B_ν.

This proves Step 2. Q.E.D.

The proof of Step 2 used Corollary 4.2(ii) to compare the exponents of $x_i/x_{i'}$ and $y_j/y_{j'}$, with typical implication $i > i' \Rightarrow \pi_{LM}(x_i) > \pi_{LM}(x_{i'})$. For Step 3 we need a similar comparison for monomials $x_i/y_{j'}$ and $y_j/x_{i'}$. Care is needed here to distinguish the order of monomials in the projection sequences from the top of V_{AB} and from the bottom of V_{LM}: the L, M exponents behave monotonically in the projection sequences of V_{AB}, and vice versa.

Lemma 5.10 *Given two monomials $m_1, m_2 \in \{x_{0\ldots k}, y_{0\ldots l}\}$, suppose that the projection sequence for V_{AB} eliminates m_1 before m_2; then*

$$\pi_{LM}(m_1) \ge \pi_{LM}(m_2). \tag{5.19}$$

Similarly, if the projection sequence for V_{LM} eliminates m_1 before m_2 then

$$\pi_{AB}(m_1) \ge \pi_{AB}(m_2). \tag{5.20}$$

See Scissors, Figure 4.2 for a picture. The proof is simply to observe that when a variable is introduced in an unprojection sequence, it appears linearly in the new tag equation at its corner. Example 4.5 provides a numerical sanity check, with the respective orders of elimination

$$V_{AB} : y_{16}, y_{15}, y_{14}, x_6, y_{13}, y_{12}, y_{11}, y_{10}, x_5, y_9, y_8, x_4, y_7, y_6, y_5, y_4, x_3, y_3, y_2, x_2;$$
$$V_{LM} : y_0, y_1, y_2, x_0, y_3, y_4, y_5, y_6, x_1, y_7, y_8, x_2, y_9, y_{10}, y_{11}, y_{12}, x_3, y_{13}, y_{14}, x_4.$$

STEP 3 *Claim 5.9 holds for all monomials $y_j y_a$ with $a = 0, \ldots, j-2$.*

First, Corollary 5.4 implies that the V_{LM} projection sequence eliminates y_a before x_{i-1}. Indeed, x_{i-1} is joined to y_j in a cross or pitchfork involving at most y_j and y_{j-1}, and these are parties to which no y_a with $a \le j-2$ is invited. Therefore Lemma 5.10 gives

$$\pi_{AB}\Big(\frac{y_a}{x_{i-1}}\Big) \ge 0. \tag{5.21}$$

As before, comparing the alleged monomial $x_i^\xi y_j^\eta m \overset{\mathbb{T}}{\sim} y_j y_a \in R(\nu)$ with the first of (5.13) gives

$$\frac{y_a}{x_{i-1}} \overset{\mathbb{T}}{\sim} x_i^{\xi-\alpha_\nu} \frac{m}{A_\nu}. \tag{5.22}$$

The proof divides into two cases.

Case 1 The projection sequence for V_{AB} eliminates x_i before y_a.

Lemma 5.10 says that $\xi - \alpha_\nu \geq 1$ is impossible in (5.22) (the lefthand side would have π_{LM} strictly smaller than the right). Thus

$$x_i^{\alpha_\nu - \xi} \frac{y_a}{x_{i-1}} \overset{\mathbb{T}}{\sim} \frac{m}{A_\nu} \quad \text{with} \quad \alpha_\nu \geq \xi, \tag{5.23}$$

and (5.21) implies that A_ν divides m.

Case 2 The projection sequence for V_{AB} eliminates y_a before x_i. This means that y_a, y_j are both contained in the interval Y_{i-1} of Lemma 5.3, and that y_a is not at the bottom:

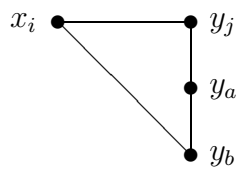

Suppose that x_i is tagged with d (or simply replace $d \leftrightarrow e$ in what follows), and write $Y_{i-1} = [b, b+d-2]$ for the interval of Lemma 5.3. Our conclusion in this case is that $\xi - \alpha_\nu < a - b + 1$ and $\equiv a - b + 1 \bmod d$, and so $\xi \leq \alpha_\nu$, and the argument of Case 1 works as before.

The proof goes as follows:

(a) For $y_a \in Y_{i-1}$

$$\pi_{LM}(y_a) = (a-b)\pi_{LM}(x_i) + \pi_{LM}(y_b) < (a-b+1)\pi_{LM}(x_i). \tag{5.24}$$

(b) On the other hand, taking π_{LM} in (5.22) gives

$$(\xi - \alpha_\nu)\pi_{LM}(x_i) \leq \pi_{LM}(y_a) - \pi_{LM}(x_{i-1}) < \pi_{LM}(y_a) \tag{5.25}$$

Therefore $\xi - \alpha_\nu < a - b + 1 \leq d - 2$.

(c) Moreover modulo $\mathbb{M}'$, we have

$$y_a \equiv \frac{x_i^{a-b+1}}{x_{i-1}} \in Q. \tag{5.26}$$

(d) Therefore in (5.22), $\xi - \alpha_\nu \equiv a - b + 1 \bmod d$.

Proof (a) follows from the tag equations for the toric variety V_{AB} at the successive y_α: as $y_{\alpha+1}$ is eliminated it has tag 1 and tag equation

$$x_i y_\alpha = y_{\alpha+1} A^{u_\alpha} B^{v_\alpha}. \tag{5.27}$$

Applying π_{LM} gives the equality in (5.24), and the inequality comes from Lemma 5.10. (b) explains itself.

When we reach the bottom of this interval, we eliminate x_i, with tag 1 and tag equation

$$x_{i-1}y_b = x_i A^{u_b} B^{v_b}. \tag{5.28}$$

Viewing this equation modulo $\mathbb{M}'$ gives $y_b \equiv x_i/x_{i-1}$, and together with (5.27) this gives the value of y_a in Q as

$$y_a \equiv y_b x_i^{(a-b)} \equiv \frac{x_i^{a-b+1}}{x_{i-1}}, \tag{5.29}$$

which proves (c).

In the coordinates of the Padded Cell Q, we know that x_{i-1} is $(0, \pm\frac{1}{e})$ and x_i is $(\pm\frac{1}{d}, 0)$. The alleged monomial tells us that $y_a \equiv x_i^{\xi-\alpha}/x_{i-1}$ modulo $\mathbb{M}'$, and (d) follows. Q.E.D.

Step 4 *Claim 5.9 holds for all monomials $x_i x_a$ with $a = 0, \ldots, i-2$.*

The prevailing assumption that $d, e \geq 2$ and $de > 4$ is necessary here; when $d = e = 2$, Claim 5.9 fails on equations of this type.

Proof We compare an alleged monomial $x_i x_a \overset{\mathbb{T}}{\sim} y_j^\eta m$ with the second expression of (5.13) as usual; move the y_j term across, this time regardless of sign, obtaining

$$y_j^{\beta_\nu - \eta} \frac{x_a}{y_{j-1}} \overset{\mathbb{T}}{\sim} \frac{m}{B_\nu}. \tag{5.30}$$

Our conclusion in this case is that $\beta_\nu - \eta - 1 > -2$ and d divides $\beta_\nu - \eta - 1$; this implies that $\pi_{AB}(m/B_\nu) \geq \pi_{AB}(x_a y_j/y_{j-1}) \geq 0$, so that B_ν divides m as required.

The proof breaks up into cases as follows; we suppose that the pristine tag on x_i is d:

The case $d > 2$, $e > 2$ The alleged monomial is $x_i x_a \overset{\mathbb{T}}{\sim} y_j^\eta m$, and we divide by the second of (5.13) to give

$$y_j^{\beta_\nu - \eta} \frac{x_a}{y_{j-1}} \overset{\mathbb{T}}{\sim} \frac{m}{B_\nu}. \tag{5.31}$$

This equation is the key at the end of the argument, but first we rewrite it trivially as

$$y_j^{\beta_\nu - \eta - 1} x_a \frac{y_j}{y_{j-1}} \overset{\mathbb{T}}{\sim} \frac{m}{B_\nu}. \tag{5.32}$$

Since $e > 2$, then as long as $i > 2$ the tag equation in V_{AB} at y_j when y_j is about to be eliminated is

$$x_{i-1} y_{j-1} \overset{\mathbb{T}}{\sim} y_j A^\bullet B^\bullet$$

for nonnegative powers of A, B that will not concern us, which we rewrite as

$$\frac{y_j}{y_{j-1}} \overset{\mathbb{T}}{\sim} \frac{x_{i-1}}{A^\bullet B^\bullet}. \tag{5.33}$$

Now (5.32) and (5.33) together give

$$y_j^{\beta_\nu-\eta-1}x_a\frac{x_{i-1}}{A^\bullet B^\bullet}\overset{\mathbb{T}}{\sim}\frac{m}{B_\nu}. \tag{5.34}$$

Since $\pi_{LM}(m/B_\nu)\geq 0$, we have

$$(\beta_\nu-\eta-1)\pi_{LM}(y_j)\geq -\pi_{LM}(x_a)-\pi_{LM}(x_{i-1}),$$

and since y_j is eliminated in the projection sequence of V_{AB} before x_a and x_{i-1}, we have $\beta_\nu-\eta-1>-2$, or in other words that

$$\beta_\nu-\eta\geq 0.$$

(The case $i=2$ is simpler: it must have $a=0$, so $\pi_{LM}(x_ix_a)=(0,*)$ by Proposition 4.1 and thus $\eta=0$; in particular $\beta_\nu-\eta\geq 0$.)

Since $d>2$, the variable x_a is eliminated before y_{j-1} in the projection sequence for V_{LM} if and only if $a<i-2$. When $a<i-2$, this projection implies that $\pi_{AB}(x_a)>\pi_{AB}(y_{j-1})$, so that $\beta_\nu-\eta\geq 0$ already gives

$$0\leq\pi_{AB}(\mathrm{LHS}(5.31))\leq\pi_{AB}(m)-\pi_{AB}(B_\nu).$$

In other words, B_ν divides m, and we are done. On the other hand, if $a=i-2$, then we can use the tag equation in V_{LM} at the point that y_{j-1} is eliminated (again using that $d>2$): namely

$$x_{i-2}y_j\overset{\mathbb{T}}{\sim}y_{j-1}L^\bullet M^\bullet \tag{5.35}$$

(for nonnegative powers of L,M that will not concern us). Writing this as

$$\frac{x_a}{y_{j-1}}\overset{\mathbb{T}}{\sim}\frac{L^\bullet M^\bullet}{y_j}$$

and substituting into (5.31) gives

$$y_j^{\beta_\nu-\eta-1}L^\bullet M^\bullet\overset{\mathbb{T}}{\sim}\frac{m}{B_\nu}.$$

Since y_j lies in a corner of the Padded Cell, this implies that d divides $\beta_\nu-\eta-1$ (which is known from above to be ≥ -1), so $\beta_\nu-\eta\geq 1$. With this, the tag equation (5.35) implies again that π_{AB} of the left-hand side of (5.31) is ≥ 0, and we conclude as before.

The case $d>2$, $e=2$ The argument proceeds almost identically, except that the tag equation in V_{AB} when y_j is eliminated is now

$$x_{i-2}y_{j-1}\overset{\mathbb{T}}{\sim}y_jA^\bullet B^\bullet$$

which we rewrite, to replace (5.33) in the argument, as

$$\frac{y_j}{y_{j-1}}\overset{\mathbb{T}}{\sim}\frac{x_{i-2}}{A^\bullet B^\bullet}.$$

The only effect is to replace occurrences x_{i-1} by x_{i-2}, and the conclusion $\beta_\nu-\eta\geq 0$ still holds.

The case $d = 2$, $e > 2$ This case differs from the others by having a cross $x_i, x_{i-1}, y_j, y_{j-1}$ at this projection bar, rather than the usual pitchfork. Nevertheless, the proof follows without change to show that $\beta_\nu - \eta \geq 0$.

But now it is easier: the cross (rather than pitchfork) implies that x_a is eliminated before y_{j-1} for any $a \leq i-2$, and the proof follows as before. Q.E.D.

6 Final remarks

This paper arose out of a study of Mori's remarkable "continued division" Euclidean algorithm [M] in the divisor class group of an extremal 3-fold neighbourhood $C \subset X$ (see also [R]). As Mori has explained to us over a couple of decades, the main result of [M] corresponds to a 2-step recurrent continued fraction $[d, e, d, \dots]$ as in our Classification Theorem 3.3. To paraphrase his argument: an extremal neighbourhood of type A has an exceptional curve $C \cong \mathbb{P}^1(r_1, r_2)_{\langle x_k, y_l \rangle}$ that is cut transversally by two divisors $\operatorname{div} x_k$, $\operatorname{div} y_l$ through the terminal points of type A. Mori's algorithm replaces these two variables successively by x_k, $x_{k-1} = Ax_k^d/y_l$, then $x_{k-1}, x_{k-2} = x_{k-1}^e/x_k$, continuing down the $d, e, d, \dots$ side of a long rectangle until it reaches x_0, y_0, that are detected by a sign reversal in their degrees. At this point, the two divisors $\operatorname{div} x_0$, $\operatorname{div} y_0$ in X intersect set-theoretically only in the curve $C \subset X$. It follows that they define a pencil $X \dashrightarrow \mathbb{P}^1$, and, in the flipping case, the flip $C^+ \subset X^+$ as its normalised graph. Our take on this is that the canonical cover of a Mori flip of Type A arises as a regular pullback from a diptych variety. We return to this in [BR4].

We comment here on the equations of V_{ABLM}, since the proof by unprojection in Section 5 deduces them by unprojection, and does not write them all out explicitly. The equations lift the toric equations of T or of V_{AB}, that are of the form $v_i v_j = \cdots$ for any pair of nonadjacent monomials on the boundary of σ_{AB}; there are thus $\binom{k+l+1}{2} - 1$ of them. Our favourites among them are the Pfaffian equations coming from magic pentagrams, which are trinomials, comparable to the binomial equations of toric geometry. These determine everything, and, as in the extended example, the full set of equations can be obtained if required. In practice, this amounts to taking a colon ideal against powers of the top monomial $x_k y_l AB$, or of the bottom monomial $x_0 y_0 LM$.

In toric geometry, we assume out of habit that Jung–Hirzebruch continued fractions $[a_1, \dots, a_k]$ have entries $a_i \geq 2$. In fact, if a tag equation $x_{i-1}x_{i+1} = x_i^{a_i}$ has $a_i = 1$ then x_i is a redundant generator. Our Classification Theorem 3.3, already implicit in Mori [M], Lemma 3.3, has output including d or $e = 1$ as regular cases. It turns out that $de = 4$ should be treated separately (see [BR2]). We used the *main case* assumption $d, e \geq 2$ and $de > 4$ in an essential way at several point in the proof of Main Theorem 1.1 in Sections 4–5. In particular, the order of unprojecting variables from top and bottom was determined by the Scissors of Figure 4.2. In the cases d or $e = 1$ with $de > 4$, we prove Theorem 1.1 in [BR3] by an argument that keeps the variable x_i tagged with 1. Allowing $d = 1$ (say) changes the shape of Scissors, and the nature of the Pretty Polytope and the Padded Cell of Section 4. In fact, the x_i marked with 1 are redundant generators, and

should be projected out before their neighbours marked with $e > 4$. This obliges us to start the proof again from scratch adopting a new order of projection; the proof then goes through in parallel with the main case.

We treat the extension $T \subset V_{AB}$ in closed form, rather than via the infinitesimal deformations of Altmann [A]. Paul Hacking observes that our diptych varieties V_{ABLM} can be seen as a variant of the construction of Gross, Hacking and Keel [GHK] in a special case. Their starting point is the *vertex of degree* n, the tent in $\mathbb{A}^n$ that is the n-cycle formed by the coordinate planes $\mathbb{A}^2_{\langle x_i, x_{i+1}\rangle}$. They construct a formal scheme that deforms this tent; their basic idea is to smooth T, replacing the local equation $x_{i-1}x_{i+1} = 0$ of T in a neighbourhood of each punctured x_i-axis by the tag equation

$$x_{i-1}x_{i+1} = A_i x_i^{a_i}, \tag{6.1}$$

where the tags a_i arise from a cycle of rational curves $D = D_1 + \cdots + D_n$ on a mirror log Calabi–Yau surface Y, D and the deformation parameters A_i play a similar role to our annotations A, B, L, M. The main difference between the two constructions is summarised by the slogan "perturbative versus nonperturbative". Whereas we work in closed form with varieties and birational unprojections, [GHK] proceed by successive infinitesimal steps: their affine pieces (6.1) are glued by formal power series expansions in affine linear transformations, specified by Gromov–Witten theory of Y, D and the Kontsevich–Soibelman and Gross-Siebert scattering diagram.

References

[A] K. Altmann, One parameter families containing three dimensional toric Gorenstein singularities, in *Explicit birational geometry of* 3*-folds*, A. Corti and M. Reid (eds), CUP 2000, 21–50

[BR2] G. Brown and M. Reid, Diptych varieties. II: Quasihomogeneous spaces, 12 pp. See `www.warwick.ac.uk/staff/Miles.Reid/Aflip/index1.html`

[BR3] G. Brown and M. Reid, Diptych varieties. III: Redundant generators, in preparation, currently 10 pp.

[BR4] G. Brown and M. Reid, Diptych varieties. IV: Mori flips of type A.

[GHK] M. Gross, P. Hacking and S. Keel, Mirror symmetry for log Calabi–Yau surfaces I, 144pp. arXiv:1106.4977

[M] S. Mori, On semistable extremal neighborhoods, in Higher dimensional birational geometry (Kyoto, 1997), Adv. Stud. Pure Math. **35**, Math. Soc. Japan, Tokyo, 2002, 157–184

[PR] S. Papadakis and M. Reid, Kustin–Miller unprojection without complexes, J. Algebraic Geom. **13** (2004) 563–577

[R] M. Reid, What is a flip? unpublished notes, 53 pp. pdf file available from `warwick.ac.uk/staff/Miles.Reid/3folds`

[dP] M. Reid, Nonnormal del Pezzo surfaces, Math Proc. RIMS **30** (1994) 695–727

[Ki] M. Reid, Graded rings and birational geometry, in Proc. of algebraic geometry symposium (Kinosaki, Oct 2000), K. Ohno (Ed.), 1–72

[R] O. Riemenschneider, Deformationen von Quotientensingularitäten (nach zyklischen Gruppen), Math. Ann. **209** (1974) 211–248

[W] Wilton, Richard II presented to the Virgin and Child by his Patron Saint John the Baptist and Saints Edward and Edmund, Diptych, Egg tempera on oak, c. 1395–9, NG4451. Google "Wilton diptych"

Gavin Brown,
Department of Mathematical Sciences, Loughborough University,
LE11 3TU, England
e-mail: G.D.Brown@lboro.ac.uk

Miles Reid,
Mathematics Institute, University of Warwick,
Coventry CV4 7AL, England
e-mail: Miles.Reid@warwick.ac.uk